



THE HONG KONG
POLYTECHNIC UNIVERSITY

香港理工大學

Pao Yue-kong Library

包玉剛圖書館

Copyright Undertaking

This thesis is protected by copyright, with all rights reserved.

By reading and using the thesis, the reader understands and agrees to the following terms:

1. The reader will abide by the rules and legal ordinances governing copyright regarding the use of the thesis.
2. The reader will use the thesis for the purpose of research or private study only and not for distribution or further reproduction or any other purpose.
3. The reader agrees to indemnify and hold the University harmless from and against any loss, damage, cost, liability or expenses arising from copyright infringement or unauthorized usage.

IMPORTANT

If you have reasons to believe that any materials in this thesis are deemed not suitable to be distributed in this form, or a copyright owner having difficulty with the material being included in our database, please contact lbsys@polyu.edu.hk providing details. The Library will look into your claim and consider taking remedial action upon receipt of the written requests.

**DEVELOPMENT OF AN ULTRASOUND
NEUROMODULATION PLATFORM
FOR PRECISE NEURONAL
STIMULATION AND REAL-TIME
MULTI-MODAL MONITORING**

WONG KIN FUNG

MPhil

The Hong Kong Polytechnic University

2022

The Hong Kong Polytechnic University

Department of Biomedical Engineering

**Development of an Ultrasound
Neuromodulation Platform for Precise
Neuronal Stimulation and Real-Time
Multi-Modal Monitoring**

WONG Kin Fung

**A thesis submitted in partial fulfilment of the
requirements for the degree of Master of Philosophy**

December 2021

CERTIFICATE OF ORIGINALITY

I hereby declare that this thesis is my own work and that, to the best of my knowledge and belief, it reproduces no material previously published or written, nor material that has been accepted for the award of any other degree or diploma, except where due acknowledgement has been made in the text.

_____ (Signed)

WONG Kin Fung _____ (Name of student)

Abstract

Ultrasound stimulation is a newly-emerging yet promising neurostimulation modality providing potential non-invasiveness and great performance in terms of spatiotemporal resolution, penetration depth and cell specificity. However, the mechanism behind is still in mist that hinders the development and translation progress. Numerous *in vivo* behaviour tests, electrophysiological recording and/or fluorescent imaging of *in vitro* or *ex vivo* samples are performed hoping to unveil how neurons respond to ultrasonic stimuli and how different biological events on cellular level merge into responses on tissue or system level. Yet without a standardized investigation strategy, it is usually hard to integrate knowledge gained. Though use of patch clamp, a powerful electro-physiology tool for single cell recording, is regarded one of gold standards in cell biology, evidence showed that patch clamp and ultrasound are in general ‘incompatible’. Many investigators adopted different strategy to overcome this ‘incompactness’ but the experimental settings were usually exclusively specific to studies. Therefore, a universal, standardized platform for general investigation purpose including patch clamp recording would be in favour to the research field.

In this study, prototypes adopting ‘direct’ and ‘circuit’ ultrasound stimulation strategy respectively were developed, which the ‘direct’ stimulation prototype possibly revealed a previously unreported ‘envelope’ phenomenon and the ‘circuit’ stimulation prototype was demonstrated to be able to serve as an ultrasound neuromodulation platform of satisfactory performance, with potential to integrate optogenetics and ultrasound neuromodulation into a single setup.

Acknowledgements

The author wants to give thanks to all the persons and organizations that have contributed to this ongoing project:

The author would like to present deep gratitude to Dr. Lei SUN, the chief supervisor, for all the advice and guidance on research methodology; appreciation also extends to research teammates, especially Mr Yong WU, for technical supports in different parts of the experiments.

Thanks also go to the University Research Facility in Behavioral and Systems Neuroscience (UBSN), The Hong Kong Polytechnic University for the provision of equipment for brain slices preparation and patch clamp recording.

Table of Contents

Abstract	i
Acknowledgements	ii
Table of Contents	iii
List of Figures	v
List of Tables	v
List of Abbreviations	vi
Chapter 1 Introduction	1
1.1 Neuromodulation	2
1.1.1 Electrical Stimuli	2
1.1.2 Magnetic Stimuli.....	3
1.1.3 Chemical Stimuli	4
1.1.4 Thermal Stimuli	5
1.1.5 Optical Stimuli.....	5
1.1.6 Acoustic/Ultrasonic Stimuli.....	6
1.2 Patch Clamp Recording.....	6
1.3 Ultrasound Neuromodulation	8
1.3.1 Fundamentals of Ultrasound.....	8
1.3.2 Overview of Ultrasound Neuromodulation.....	13
1.3.3 Mechanism.....	14
1.4 Aims of Study.....	14
Chapter 2 Ultrasound Neuromodulation Platform Prototype I – Direct Stimulation with Confined Transducer	16
2.1 Materials and Methods	16
2.1.1 Ultrasound Stimulation Platform with Patch Clamp System.....	16
2.1.2 Ultrasound Transducer Characterization	16
2.1.3 Animal Treatment	17
2.1.4 Brain Slices Preparation.....	18
2.1.5 Electrophysiology Recording (Patch Clamp).....	18
2.1.6 Ultrasound Stimulation	19
2.2 Results	20
2.2.1 Ultrasound Stimulation Platform with Patch Clamp System.....	20
2.2.2 Ultrasound Transducer Characterization	21
2.2.3 Ultrasound Stimulation Evaluation.....	22
2.3 Discussion	25
Chapter 3 Ultrasound Neuromodulation Platform Prototype II – Stimulation through Neuronal Circuit	27

3.1 Materials and Methods	27
3.1.1 Ultrasound Stimulation Platform with Patch Clamp System	27
3.1.2 Ultrasound Transducer Characterization	27
3.1.3 Animal Treatment	28
3.1.4 Brain Slices Preparation.....	29
3.1.5 Fluorescence Imaging	29
3.1.6 Electrophysiology Recording (Patch Clamp).....	30
3.1.7 Ultrasound Stimulation	30
3.2 Results	31
3.2.1 Ultrasound Transducer Characterization	31
3.2.2 Ultrasound Stimulation Platform with Patch Clamp System.....	32
3.2.3 Ultrasound Stimulation Evaluation.....	35
3.2.4 Optical Stimulation Evaluation.....	39
3.3 Discussion	40
Chapter 4 Conclusion	43
References	44

List of Figures

Figure 1 Particle movement under effect of longitudinal and transverse waves	9
Figure 2 Graphical illustration of typical time-related ultrasound parameters.....	10
Figure 3 Numerical determination of the ultrasonic field generated by a circular piston	11
Figure 4 Sample acoustic profile on the plane of tissue under sonication.....	12
Figure 5 The developed ‘direct’ ultrasound stimulation platform prototype	21
Figure 6 Acoustic output calibration of the confined transducer.....	22
Figure 7 Unexpected sinusoidal ‘envelope’	24
Figure 8 The induction of ‘envelope’ is medium-mediated.....	25
Figure 9 Acoustic output calibration of the custom-made needle transducer	32
Figure 10 The developed ‘circuit’ ultrasound stimulation platform prototype	34
Figure 11 Fluorescence image of EGFP (MscL) at VTA region.....	35
Figure 12 No observable ion channels activation by ultrasound under same site recording at NAC	38
Figure 13 Ion channels activated by ultrasound under same site recording at VTA.....	37
Figure 14 Ion channels activated by ultrasound via ‘circuit’ strategy	36
Figure 15 Sensitization of neurons at VTA to optical stimulation	40

List of Tables

Table 1 Sample denotation system for ultrasound pressure and intensity.....	12
---	-----------

List of Abbreviations

ACSF	artificial cerebrospinal fluid
AP	action potential
BBB	blood brain barrier
CES	cranial electrotherapy stimulation
ChR2	channelrhodopsin-2
CNS	central nervous system
CW	continuous wave
DIO	double-floxed inverse open reading frame
DoF	degree-of-freedom
EGFP	enhanced green fluorescent protein
f	frequency
HIFU	high intensity focused ultrasound
LIUS	low intensity pulsed ultrasound
MscL	large-conductance mechanosensitive ion channel
NAC	accumbens nucleus
NMDG	N-methyl-D-glucamine
P_{sptp}	spatial-peak temporal-peak acoustic pressure
T	period
t1	pulse width
t2	pulse interval
t3	burst duration
t4	burst interval
tACS	transcranial alternating current stimulation
tDCS	transcranial direct current stimulation

tES	transcranial electrical stimulation
tPCS	transcranial pulsed current stimulation
tRNS	transcranial random noise stimulation
VTA	ventral tegmental area

Chapter 1 Introduction

The nervous system is one of the most complex and important system in animal, providing information receiving, processing and signalling, and serving as control unit of voluntary events and mediator of involuntary events. For years, the central nervous system (CNS), especially the brain, has been under focus of scientific research. With advanced technologies in anatomy and physiology, scientists are able to observe and even manipulate CNS function by different means. However, the mechanism behind various CNS functions is yet to be understood completely. Strategies such as *in vivo* animal behaviour tests, electrophysiological recording and/or fluorescent imaging on *in vitro* or *ex vivo* samples are commonly adopted to investigate single neuron response towards stimuli, or signal propagation and feedback mechanism within neural circuits, in hope of decoding the complicated activities of the CNS. Usually, for *in vivo* behaviour studies, stimulation would be delivered to neurons with less spatial selectivity or greater area under effect, while for *in vitro* or *ex vivo* studies, stimulation would be delivered as precise as possible with smaller area under effect. Though behaviour-type of investigation can provide more direct information that can be translated into clinical application more easily, results are typically strictly specific to such input-output correlation that causation relationship or the mechanism behind can hardly be determined, in other words, much more studies might be needed to develop a general but thorough understanding to the technique itself in clinical settings, which efficiency and safety are two major concerns. In this context, selective and localized stimulation followed by cellular or sub-cellular level monitoring is desired. To obtain convincing conclusions, strategies and parameters of both stimulation delivery and response recording should be carefully designed. Key considerations for a general

investigation system include, but not limited to, cell specificity, spatiotemporal resolution, penetration depth, and absence of potential adverse bioeffect.

1.1 Neuromodulation

Neuromodulation, a manual alteration of neural activities through targeted delivery of extrinsic stimuli, has been on stage of clinical application for decades. Since the discovery of action potential (AP) in nervous system, electricity has been playing an important role in neuroscience and thus became the very first candidate for neuromodulation. In the past decades, more and more stimuli of different physical nature have been shown to be capable of altering neuron excitability, for example, electrical, magnetic, chemical, thermal, optical, and acoustic/ultrasonic stimuli, and numerous of *in silico*, *in vitro*, *ex vivo* and *in vivo* experiments have been conducted. Yet, none of the modulation modalities has been shown to be ‘perfect’ which each of them was optimized and best adopted in different scenario. A brief summary of the modalities is shown as follow:

1.1.1 Electrical Stimuli

One of the fundamental ‘messengers’ in nervous system is AP, electrical pulses traveling along nerves without actual electrical current at the direction. Since discovery of AP, electricity has been playing important roles in neuroscience and without doubt, electrical stimulation would be one of the first modalities scientists applied for neuromodulation. Electrical stimuli generally provide excellent temporal resolution, but often pose challenge to investigators to achieve great spatial resolution or selectivity. Traditional electrical neuromodulation methods involve electrode implants in target region to deliver trains of electrical current of pre-set pattern, at a regular time interval or upon detection of certain physiological events. Since improving spatial resolution simply by reducing electrode size would increase electric resistance, trading

off stimulation efficiency, recent research of stimulation tools mainly focuses on use of advanced materials for electrode fabrication (de Asis Jr, Leung, Wood, & Nguyen, 2009; Park et al., 2018). Modern alternatives in the family of transcranial electrical stimulation (tES) such as transcranial direct current stimulation (tDCS), transcranial alternating current stimulation (tACS, also known as cranial electrotherapy stimulation, CES), transcranial pulsed current stimulation (tPCS) and transcranial random noise stimulation (tRNS), as the names suggest, non-invasively apply different patterns of current trains through cranium to stimulate neurons of CNS (Guleyupoglu, Schestatsky, Edwards, Fregni, & Bikson, 2013), for the price of further reduced spatial specificity. Evidence shows tES is effective in mood disorder treatment (Rosa & Lisanby, 2012), motor-related rehabilitation (Yavari, Jamil, Samani, Vidor, & Nitsche, 2018) and cognitive function improvement (Chang, Lane, & Lin, 2018), where large area of brain circuit might be responsible.

1.1.2 Magnetic Stimuli

In classical physics, electromagnetism is one of the four fundamental interactions in nature and thus, electricity and magnetism often come in pair in various scenarios. By applying a time variant magnetic field, a non-zero electric field, usually in form of loops of electric current called eddy current or Foucault's current, would be induced within the effector. Such electromagnetic technique, when applied on neuromodulation, is commonly known as magnetic neuromodulation or magnetic nerve stimulation (Eaton, 1991). In contrast to electrical neuromodulation, instead of direct current application, endogenous electric current is induced by magnetic pulses delivered non-invasively. Since magnetic field can readily penetrate the scalp and skull, magnetic neuromodulation can achieve relatively great penetration depth. Though localized effect can be obtained by carefully designed magnetic field generator and

stimulation protocol, spatial resolution and cell selectivity might just be acceptable (Bijsterbosch, Barker, Lee, & Woodruff, 2012; Janssen, Oostendorp, & Stegeman, 2014; Rossini et al., 2015).

1.1.3 Chemical Stimuli

Neural activities depend heavily on chemicals, from basic AP generation within single neuron cell to complex cognitive decision of the CNS. AP is an electricity event by nature but generation and travel of AP is more chemical than electrical. The three main stages in AP generation: depolarization, repolarization and hyperpolarization are results of in- or outflow of charged ions; neurons are not physically connected for AP to travel along that certain chemical messengers, termed neurotransmitters, are responsible to diffuse across the 'gap' (synaptic cleft) that promote or inhibit AP generation on the postsynaptic neuron. In other words, changing any of the conditions can significantly alter the primary function of neuron cells. Yet, presence of blood brain barrier (BBB) makes conventional oral intake or intravenous injection inadequate to deliver neuro-drugs to the target regions. Various technologies have been developed to overcome the physiological barrier, either by-passing or forcing through. One of the iconic by-passing strategies is epidural or intrathecal drug delivery system, utilizing cerebrospinal fluid that fills the space in CNS as carrier of drugs; (Fowler et al., 2020) with the help of external forces such as ultrasound, BBB could be temporarily opened, allowing diffusion of drugs from blood to target region in CNS. Under either strategies, spatiotemporal resolution and selectivity remain major drawback that depend heavily on natures of the chemical used (Pardridge, 2011), which could be improved with advanced synthetic or packaging technology to enhance sustainable delivery and minimize off-target effect.

1.1.4 Thermal Stimuli

Temperature change affects not only particle movement and chemical reaction, but also causes change in various physical properties of cell membrane, both lipid bilayer and ion channels, which in turn alter the activation/deactivation dynamics of AP (Duke et al., 2013). Despite any energy delivery means that could be rapidly controlled in time domain to provide transient heating effect could be utilized theoretically, magnetothermal, photothermal and high intensity focused ultrasound (HIFU) are typical candidates. Unlike magnetothermal, which relies on micro- or nano-transducers to convert incident RF radiation into heat, photothermal and HIFU can solely heat the target cell with relatively high spatial resolution. Yet, micro- or nano-technology could be combined to further enhance spatiotemporal resolution and effective intensity threshold. (Paviolo & Stoddart, 2017) Still, tissue damage remains main concern for thermal neuromodulation since effective threshold and damaging threshold might be close in certain scenario (Richter, Matic, Wells, Jansen, & Walsh, 2011). Further development in nanotechnology might be beneficial to optimizing the technique in terms of efficiency, specificity, and safety. (Yang & Park, 2021)

1.1.5 Optical Stimuli

Optical neuromodulation, sometimes referred as optogenetics, is a fast-growing, well-established technology in neuroscience that combines ‘optics’ and ‘genetics’. By carefully designed photosensitive ion channel overexpression on target neurons through proper genetic vector, gain- or loss-of-function of well-defined neural activities can be achieved on living tissues (Deisseroth et al., 2006) with excellent cell specificity and relatively high temporal resolution, due to cell type specific transfection and relatively fast response of ion channels. On top of these, precise control of illumination on transfected tissue using specific wavelengths of light heavily

determines precision and spatiotemporal resolution of cell, circuit or animal-wise activity modulation. Though being ‘Method of the Year 2010’ (Pastrana, 2011), optogenetics generally suffers from intrinsic drawbacks of the necessity of invasive surgery for gene delivery and poor penetration depth of light in most biological tissues. Recent research showed possibility of deep brain stimulation without implant nor surgery (Chen et al., 2021), efforts remain required to optimize such strategy.

1.1.6 Acoustic/Ultrasonic Stimuli

Mechanical stimulation can be applied in forms such as compression, stretching, sheer stress that deforms cell body (Brown, 2000), and eventually causes depolarization and AP firing through different biophysical pathways. Many systems have been developed to apply different types of mechanical loading to cells or tissue *in vitro* or *ex vivo* (Brown, 2000), ultrasound is usually adopted *in vivo* and in a number of *in vitro* settings. Ultrasound waves experience limited scattering in most biological tissues and is capable for transcranial stimulation, thus providing potential non-invasiveness, great penetration depth and great spatiotemporal resolution. Though the underlying biophysical principle is not well understood (Blackmore, Shrivastava, Sallet, Butler, & Cleveland, 2019; Kamimura, Conti, Toschi, & Konofagou, 2020), numerous studies have shown its effectiveness on both central and peripheral nervous systems in different vertebrates (Blackmore et al., 2019). Uncertainty upon safety and effective parameters greatly hinders translation to clinical application.

1.2 Patch Clamp Recording

Patch clamp, first reported in 1970s, is a powerful electro-physiology tool capable of single cell, single ion channel recording (Neher & Sakmann, 1976) which in turn contributes to Nobel Prize winning discoveries concerning “the function of single ion channels in cells” (Neher & Sakmann, 1991). Fundamentally, a properly shaped glass

pipette with opening in micrometre scale is brought to the cell membrane with gentle suction, forms a tight seal around and isolates that particular portion of cell membrane and ion channels on top from the extracellular microenvironment, thus cross membrane potential or current change could be recorded.

Back in 1990s, inventors of the tool reported three forms of patch clamp recording techniques (Neher & Sakmann, 1992): Firstly 'cell-attached patch' that being the fundamental recording approach; secondly 'whole-cell patch' that after formation of the tight seal against cell membrane, further suction was applied to 'break' the isolated membrane while the seal remains, thus enabling recording of multi-channel activities across the whole cell; and thirdly 'channel isolated patch' that after formation of the tight seal against cell membrane, the cell membrane around is ruptured by slight retraction of the pipette, detaching the isolated portion from the cell body. Depending on the surrounding medium or if further action is taken, this technique derives into 'outside-out patch' and 'inside-out patch', which in the former variation the open ends of the detached fragment fuse back to form a vesicle structure, leaving the extracellular surface remains exposed to extracellular medium, while in the latter, intracellular surface is exposed instead thus enabling manipulation of intracellular microenvironment of single ion channel. Both variations allows investigators to examine response of ion channel under precisely controlled environment with minimum effect of other organelle. On top of these, alternate to 'whole-cell patch', named 'perforated patch', was also reported (Horn & Marty, 1988): in stead of complete rupture of the isolated cell membrane, antimicrobials were added into the pipette's internal solution to create small pores on the membrane, allowing electrophysiology recording on whole cell with limited disturb to intracellular microenvironment.

In more modern era, more advancements in patch clamp techniques have been made and it is more widely applied in different research areas, such as neuron genotype-phenotype matching (Lipovsek et al., 2021) and drug discovery (Obergrussberger, Friis, Brüggemann, & Fertig, 2021). Yet, fundamental requirement of a constant seal sometimes hinders involvement of patch clamp in several research scenarios, for example, scenarios involving ultrasound application. Conventional strategy of ultrasound application is often reported ‘incompatible’ with patch clamp recording (Collins & Mesce, 2020; Lin et al., 2018; Prieto, Firouzi, Khuri-Yakub, & Maduke, 2018; Qiu et al., 2019; Tyler et al., 2008) that the giga-ohm tight seal might become unstable or ‘false positive’ response might be captured.

1.3 Ultrasound Neuromodulation

1.3.1 Fundamentals of Ultrasound

Ultrasound can be loosely defined as sound wave of frequency beyond than human audible range, or more precisely, mechanical wave of frequency no less than 20 kHz. In most scenarios, ultrasound exists as longitudinal wave that particles under effect oscillates along wave propagation direction (Fig. 1), producing compression and rarefaction along the way together with oscillation of local pressure. By tracing a single particle under sonication, the magnitude and direction of motion can be plotted and visualized as a function of time similar to that of transverse wave.

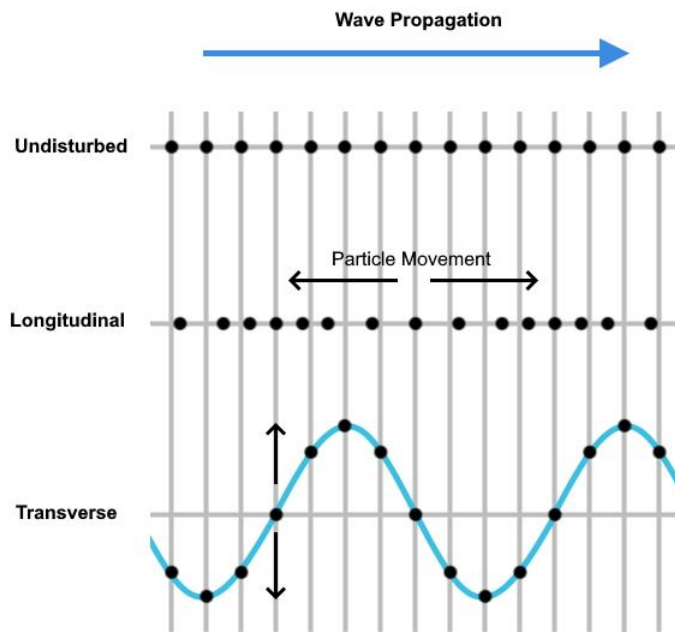


Figure 1. Particle movement under effect of longitudinal and transverse waves.

In biological applications, it is important to report parameters of stimulation used accurately, precisely, and quantitatively. Typically, parameters of an ultrasonic setup can be grouped into time-related, space-related, and energy-related (or pressure-related). Since ultrasound propagation involves particle oscillation, one important parameter is frequency (f), or equivalently, period (T), indicating how fast the oscillation is. Besides, to induce different bioeffects, certain ON/OFF sequence might be adopted, which is usually denoted by parameters pulse width, pulse interval, burst duration, and burst interval, sometimes referred as t_1 , t_2 , t_3 , and t_4 respectively. Fig. 2 shows a graphical illustration of the parameters. Under this setting, usually referred as pulsed ultrasound, one may imagine sonication be governed by one or two sets of ON/OFF cycles. If sonication is applied continuously without such gating in time, the sonication is usually referred as in continuous wave (CW) mode.

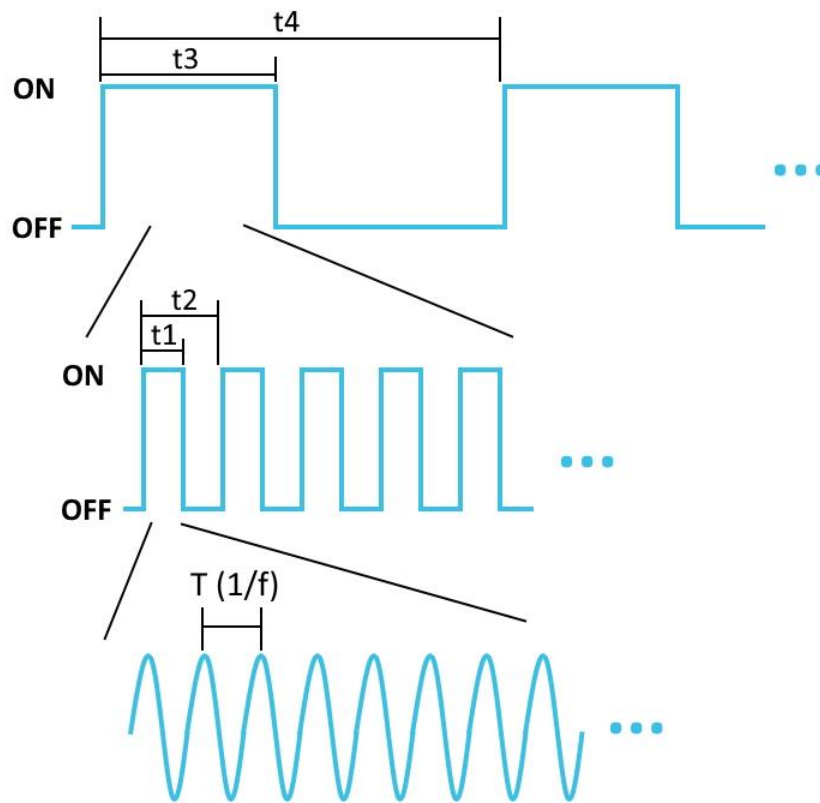


Figure 2. Graphical illustration of typical time-related ultrasound parameters.

Besides variation across time, due to wave nature of ultrasound, interference and attenuation make oscillation amplitude varies at different spatial positions (Fig. 3), which the former is more dominant at locations close to the transducer (near field) and the latter is more dominant at more distant locations (far field). The acoustic profile is relatively uniform in far field but might be messy in near field, it is suggested to locate target cell/tissue at locations within far field. However, it is not rare that adopting experimental positioning of sonication in far field is deemed impractical because the length of near field (also known as Fraunhofer distance) is determined by frequency of ultrasound (precisely speaking, wavelength of ultrasound in the medium) and dimension of ultrasound generating element used, which could extend to several centimetres:

$$d = \frac{(D/2)^2}{\lambda} = \frac{fD^2}{4v}$$

where d is the length of near field (cm), D is the diameter of the transducer (cm), λ is the wavelength of ultrasound in the medium (cm), f is the frequency of ultrasound (Hz), v is the speed of ultrasound in the medium (cm/s).

Thus, especially when near field sonication is adopted, reporting the transducer-target positioning and/or acoustic profile (Fig. 3a & 4) is crucial for more repeatable and translatable results.

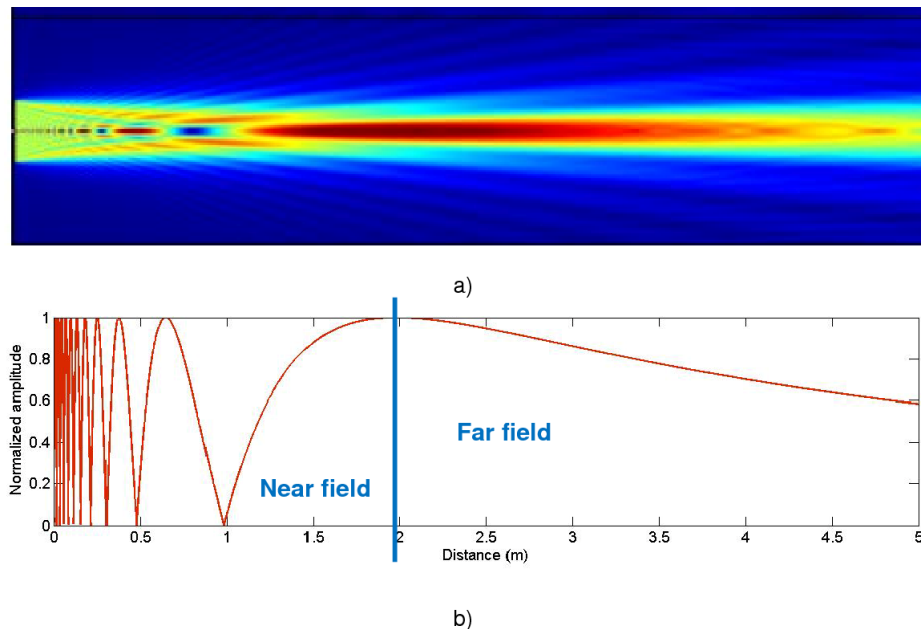


Figure 3. Numerical determination of the ultrasonic field generated by a circular piston. **(a)** 2D ultrasonic field in free field; **(b)** 1D ultrasonic intensity along the axis.

Reprinted from “Ultrasonic field generated by different airborne power ultrasonic transducers with extensive radiators” by Andrés, R. R., Acosta, V. M., & Riera, E., 2017, Paper presented at the Tecniacústica 2017: 48º Congreso Español de Acústica; Encuentro Ibérico de Acústica; European Symposium on Underwater Acoustics Applications; European Symposium on Sustainable Building Acoustics: A Coruña 3-6 Octubre 2017.

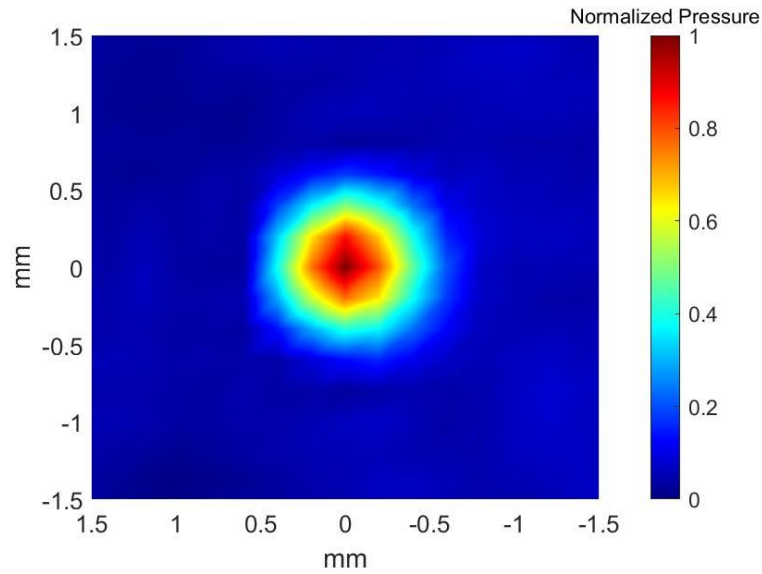


Figure 4. Sample acoustic profile on the plane of tissue under sonication. (replica of **Figure 6b**)

It is not hard to notice that numerical value of pressure or intensity of ultrasound sonication is a function of time and space, systematic denotation is necessary to prevent confusion and/or misunderstanding. Usually, a 4-character system is adopted:

Table 1. Sample denotation system for ultrasound pressure and intensity.

Space	Time	
Spatial Peak	Temporal Peak	Spatial Peak-Temporal Peak (SPTP)
Spatial Average		Spatial Average-Temporal Peak (SATP)
Spatial Peak	Pulse Average	Spatial Peak-Pulse Average (SPPA)
Spatial Average		Spatial Average-Pulse Average (SAPA)
Spatial Peak	Temporal Average	Spatial Peak-Temporal Average (SPTA)
Spatial Average		Spatial Average-Temporal Average (SATA)

where spatial peak means the greatest value measured at a single point within the beam (usually at the centre), spatial average means the average value across the beam,

temporal peak means the greatest value recorded across the sonication period, pulse average means the average value across only the pulse duration (t_1), temporal average means the average value across the whole sonication period.

1.3.2 Overview of Ultrasound Neuromodulation

Although ultrasound neuromodulation is a newly-emerging neurostimulation modality, pilot study could be dated as far back as in early 20th century. Harvey (1929) was one of the first investigators successfully demonstrated ultrasound-induced electric signal on frog's heart immersed in Ringer's solution. While it is long known that ultrasound could reversibly modulate neural activities (Shealy & Henneman, 1962; Young & Henneman, 1961), it is until recent that low intensity pulsed ultrasound (LIUS) is proven capability for neurostimulation through non-thermal mechanism (Tyler et al., 2008). The finding is later strengthened by Dallapiazza et al. (2017) that no temperature increase can be observed by magnetic resonance thermometry upon successful LIUS induced neuronal response. As ultrasound travels in biological tissues with limited dispersion or scatter, together with breakthroughs ultrasound focusing technology in focusing, non-invasive, localized stimulation with great temporal resolution and penetration depth is achievable (P. Wang, Zhang, Yu, Smith, & Feng, 2019). Besides, several groups have reported a number of ion channels activatable by ultrasound stimulation (Kubanek, Shukla, Das, Baccus, & Goodman, 2018; Oh et al., 2019; Qiu et al., 2019), which some of them have been genetically decoded. By overexpressing such ion channels to target cells, or introducing acoustic enhancing micro- or nanoparticles targeting characteristic ion channels, cell specificity can significantly be enhanced. Up to date, there is only one reported case showing adverse effect directly linked to ultrasound stimulation: minor microhemorrhages were

observed from V1 areas of sheep receiving stimulation of high pulse repetition frequency (Lee et al., 2016).

1.3.3 Mechanism

Ultrasound is known to be capable of inducing various bioeffect depending on the sonication parameters used (Focused Ultrasound Foundation, 2015), the biophysical mechanism behind, especially neuromodulation, might not be fully understood. Hypotheses have been suggested, while some being regarded less likely or of minor effect, the rest remain debatable that no solid conclusion can be drawn yet.

Plausible hypotheses include acoustic radiation force, a low frequency mechanical force translated from higher frequency oscillation; intramembrane stable cavitation, where gas bubble or void, induced under sufficiently high negative pressure, oscillates along the carrier mechanical wave; sonoporation, change in membrane permeability or creation of physical pores that allows ion in- or outflow; and flexoelectricity, change of membrane capacitance due to lipid bilayer deformation or change of its conformational state which in turn induces depolarization (Sassaroli & Vykhodtseva, 2016). Numerous research works have been conducted in attempt to build an optimal model for ultrasound neuromodulation, the effort occasionally provides seemingly contradictory evidences (Baek, Pahk, & Kim, 2017; Blackmore et al., 2019; Kamimura et al., 2020; Rezayat & Toostani, 2016; S. Wang et al., 2020). Yet, Kamimura et al. (2020) suggested the issue be associated with potential variability in experimental conditions that detailed standardization is needed to reconcile present findings.

1.4 Aims of Study

Cell specificity, spatiotemporal resolution, penetration depth, and absence of potential adverse bioeffect are members of major considerations while designing a

neuromodulation tool. Ultrasound neuromodulation, on one hand, shows prompt potential in all these areas thus is considered one of optimal modality; on the other hand, lack of throughout understanding in its mechanism and yet to be established effective, safe stimulation protocols require further effort before this technique can be well-translated into clinical applications.

Several mechano-sensitive machineries have been shown to play important roles in cellular response towards ultrasound with their actions being instantaneous, an investigation tool with real-time recording, precise stimulation and flexibility in stimulation parameters is essential for model construction and evaluation. Many groups have performed investigation on ultrasound-cell interaction using custom-made systems, yet the developed systems are generally study-specific. Development of an optimal, convenient and reliable ultrasound neuromodulation platform for precise neuronal stimulation and real-time multi-modal monitoring fulfilling general investigation purpose remains in need.

This study aimed to develop an ultrasound neuromodulation platform for precise neuronal stimulation and real-time multi-modal monitoring, as a standardized protocol and/or method. Two prototypes adopting, respectively, ‘direct’ and ‘circuit’ stimulation strategy were developed. Feasibility and performance of the developed platforms as an investigation platform was evaluated on mechanosensitive and photosensitive ion channels expressing murine brain slices.

Chapter 2 Ultrasound Neuromodulation Platform Prototype I –

Direct Stimulation with Confined Transducer

In this Chapter, a stimulation platform equipped with transducer confined by self-fabricated acoustic guide was developed, aiming to locally stimulate target neuron with visual aid of microscope. Brain slices sensitized with mechanosensitive ion channel MscL at VTA were prepared for performance test.

2.1 Materials and Methods

2.1.1 Ultrasound Stimulation Platform with Patch Clamp System

A 5 degree-of-freedom (DoF) micromanipulating platform for ultrasound transducer was constructed by assembling a 3-D manual micromanipulator (MM 33 with clamp, Märzhäuser Wetzlar, Germany), a 1-D goniometer (KSMG10-65, Zolix, China) and a rotation stage (RSM82-1A, Zolix, China) and fixed on a fixed stage microscope (BX51W1, Olympus, Japan) together with a motorized micromanipulator for patch clamp (MP-285, Sutter Instrument, USA). Narrow cone-shaped acoustic guide was fabricated out of 10 μ L pipette tip sealed with polyethylene film, filled with deionized, degassed water and fixed upon custom-made needle transducer, which was then fixed on the 5-DoF micromanipulating platform.

2.1.2 Ultrasound Transducer Characterization

The custom-made needle transducer equipped with acoustic guide was immersed in a large tank of deionized, degassed water, together with a hydrophone (HGL0200, ONDA, USA; preamplifier: AG2010, ONDA, USA) installed on a 3-D translation stage (controller: XPS-D, Newport, USA; stage: M-ILS150CCHA, Newport, USA; XML210, Newport, USA). A combo of two function generators (Tektronix AFG3251, Agilent Technologies, USA; DG4102, Rigol, China) and a RF power amplifier (A075,

Electronics & Innovation Ltd, USA) was used to drive the ultrasound transducers. To determine the driving voltage input and acoustic output relationship, the hydrophone was aligned with the centreline of the transducer, separated by a distance similar to that of the patch clamp experimental setup, waveforms under varying driving voltage were captured using oscilloscope (DS4024, Rigol, China) with matching input impedance; for the acoustic profile, upon finish of hydrophone-transducer alignment, a LabVIEW (National Instruments, USA) programme in sync with the function generators and an ADC board (PCI-5112, National Instruments, USA) was used to perform point-by-point 2D scanning of a pre-assigned area and step length. Waveforms at each scan point were captured and saved by the ADC board. In both tests, values of corresponding acoustic pressure were converted from the captured waveforms with pre-calibrated coefficient of hydrophone-preamplifier set provided by manufacturer.

2.1.3 Animal Treatment

C57BL/6 mice aged approximately 6 weeks were anesthetized with ketamine and xylazine (50 mg/kg and 15 mg/kg respectively) followed by shaving the skin above skull. Using a stereotaxic apparatus (RWD, China), a craniotomy hole was drilled to allow injection. The coordinates used for VTA were AP -3.5 mm, ML 0.4 mm, DV -4.2 mm. Injection site received 1 μ L of rAAV-hSyn-MSCL-G22S-F2A-EYFP-WPRE-pA virus at 0.1 μ L/min, followed by a 10-minute pause. The pipette was then retracted slowly, including a 5-minute pause at the halfway point. The puncture site was then disinfected and sutured, and the mice were returned to their housing areas for a recovery period no less than 3 weeks.

2.1.4 Brain Slices Preparation

Brain slices were prepared with reference to Ting et al. (2018): anesthetization was performed on the treated mice using ketamine and xylazine (50 mg/kg and 15 mg/kg respectively), followed by heart perfusion using N-methyl-D-glucamine (NMDG) artificial cerebrospinal fluid (ACSF) (92 mM NMDG, 2.5 mM KCl, 1.25 mM NaH₂PO₄, 30 mM NaHCO₃, 20 mM HEPES, 25 mM glucose, 5 mM sodium ascorbate, 2 mM thiourea, 3 mM sodium pyruvate, 10 mM MgSO₄, 0.5 mM CaCl₂, pH 7.3~7.4 using HCl). Animal euthanasia was performed by cervical dislocation. Brains were then quickly removed and chilled in ice-cold NMDG ACSF well oxygenated with 95% O₂ + 5% CO₂. Sagittal slices (300 μm) were then cut using a semiautomatic vibrating blade microtome (VT1200, Leica Biosystems, USA) and subsequently incubated for 10 minutes at 35°C. The slices were then transferred to a light-shielding storage chamber filled with oxygenated holding ACSF (92 mM NaCl, 2.5 mM KCl, 1.25 mM NaH₂PO₄, 30 mM NaHCO₃, 20 mM HEPES, 25 mM glucose, 5 mM sodium ascorbate, 2 mM thiourea, 3 mM sodium pyruvate, 2 mM CaCl₂, 2 mM MgSO₄, pH 7.3–7.4 using NaOH, oxygenated with 95% O₂ + 5% CO₂) at room temperature. A recovery period no less than 60 minutes was allowed before patch clamp recordings.

2.1.5 Electrophysiology Recording (Patch Clamp)

Glass pipettes used were pulled from glass capillary tube (Vitrex, Modulohm A/S, Denmark) using Flaming/Brown micropipette puller (P-1000, Sutter Instrument, USA). The pipettes were filled with internal solution (138 mM KCl, 10 mM NaCl, 1 mM MgCl₂, 10 mM HEPES with D-manitol compensated for 290 mOsm) prior patch clamp recordings. Patch clamp recordings were done using HEKA patch clamp system (EPC 10 USB, HEKA Elektronik, Germany; software: PATCHMASTER, HEKA Elektronik, Germany) under visual aid of differential interference contrast microscopy

(BX51WI, Olympus, Japan; digital camera: 01-PRIME-BSI-EXP, Teledyne Photometrics, USA). Brain slices were bathed in recording ACSF (124 mM NaCl, 2.5 mM KCl, 1.25 mM NaH₂PO₄, 24 mM NaHCO₃, 12.5 mM glucose, 2 mM CaCl₂, and 2 mM MgSO₄, oxygenated with 95% O₂ + 5% CO₂) under perfusion. Brain region was identified by visual inspection and cell type was confirmed by characteristic waveforms under voltage step stimulation (-100 mV to 100 mV). After formation of whole-cell giga-ohm seal, holding voltage was set at -60mv. Cell activities in term of inward current were recorded using continuous passive voltage-clamp under gap-free recording mode and sampling rate 1 kHz.

2.1.6 Ultrasound Stimulation

To evaluate effect of ultrasound stimulation, the tip of acoustic guide was placed near the glass pipette with an angle, pointing towards the targeting neuron. The same combo of two function generators (Tektronix AFG3251, Agilent Technologies, USA; DG4102, Rigol, China) and a RF power amplifier (A075; Electronics & Innovation Ltd, USA) as in ultrasound transducer calibration was used to drive the ultrasound transducers, generating single-tone bursts of varying spatial-peak temporal-peak acoustic pressure (P_{sptp}), pulse width (t1), pulse interval (t2), burst duration (t3), and burst interval (t4).

2.2 Results

2.2.1 Ultrasound Stimulation Platform with Patch Clamp System

Since alignment of the ultrasound transducer greatly influence the acoustic profile at the recording chamber, to maximize tunability of the system, a 5-DoF manual micromanipulating platform for ultrasound transducer was constructed and fixed on a fixed stage microscope for patch clamp recording (Fig. 5a,b). A custom-made needle transducer equipped with a narrow cone-shaped acoustic guide (Fig. 5c) could be fixed on top, allowing fine-tuning for optimal micropipette-cell-transducer alignment.

To set the system for experimental validation, the transducer was tilted to avoid standing wave, which could alter the acoustic pressure at a certain point from near zero to up to double the original value. The fine-tuning process was visually aided by microscope since the micropipette, acoustic guide and brain slice sample were able to be seen in a single field of view (Fig. 5d).

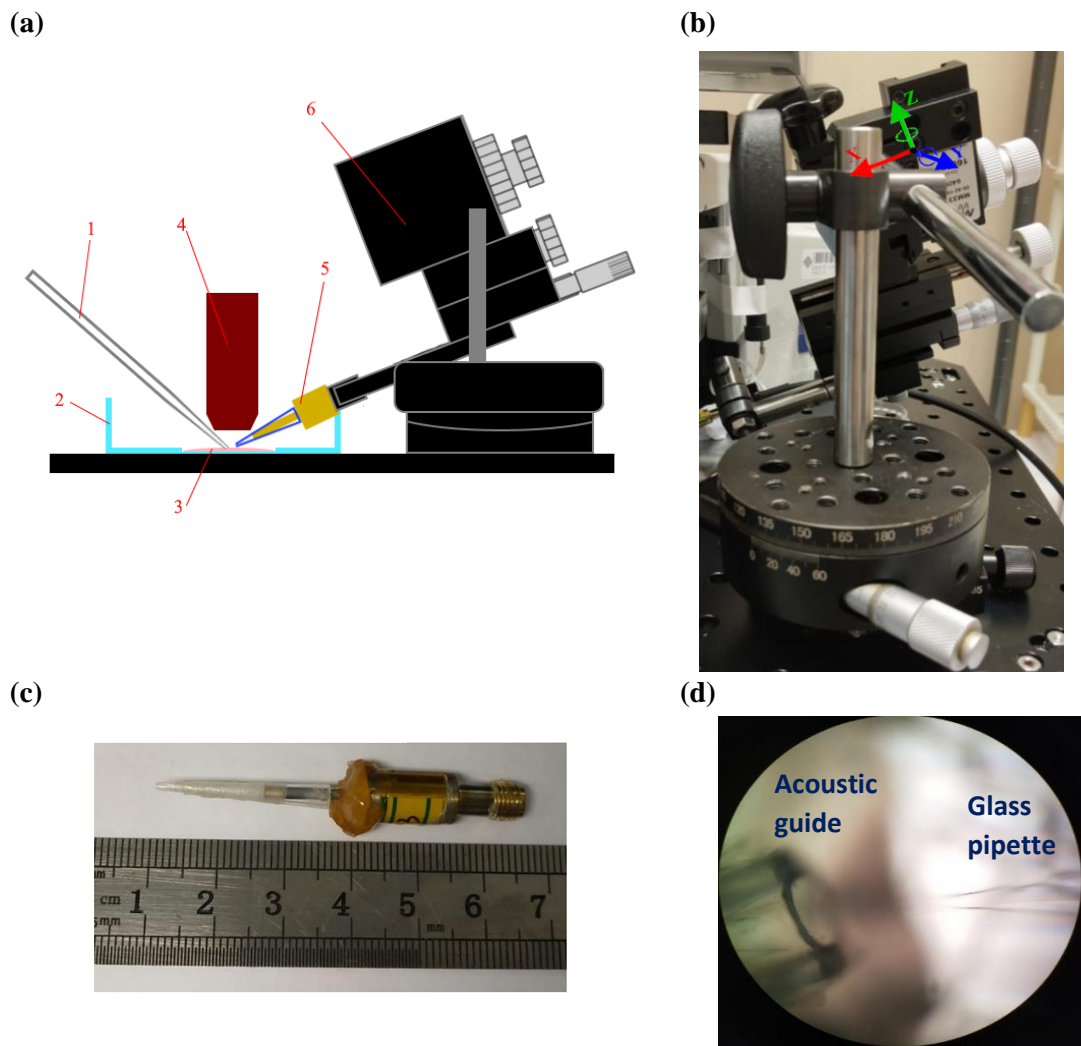


Figure 5. The developed ‘direct’ ultrasound stimulation platform prototype. **(a)** Schematic illustration of the developed system. (1) patch pipette; (2) record chamber modified from confocal dish; (3) tissue sample (brain slice); (4) microscope objective; (5) ultrasound transducer; (6) 5-DoF micromanipulating platform; **(b)** The 5-DoF micromanipulating platform; **(c)** Demonstration of the custom-made needle transducer equipped with acoustic guide; **(d)** Demonstration of tip of acoustic guide and glass pipette being visible under microscope.

2.2.2 Ultrasound Transducer Characterization

To quantify the acoustic output, hydrophone measurement was performed in a large tank of deionized, degassed water (Fig. 6a). Measurement was carried out near the tip of acoustic guide, where targeting cell was expected to locate. Point-by-point 2D

scanning (Fig. 6b) showed that the acoustic beam was slightly less than 1mm in diameter. Single-point measurement (Fig. 6c) was carried out at the centre of acoustic beam to map driving voltage to P_{sptp} .

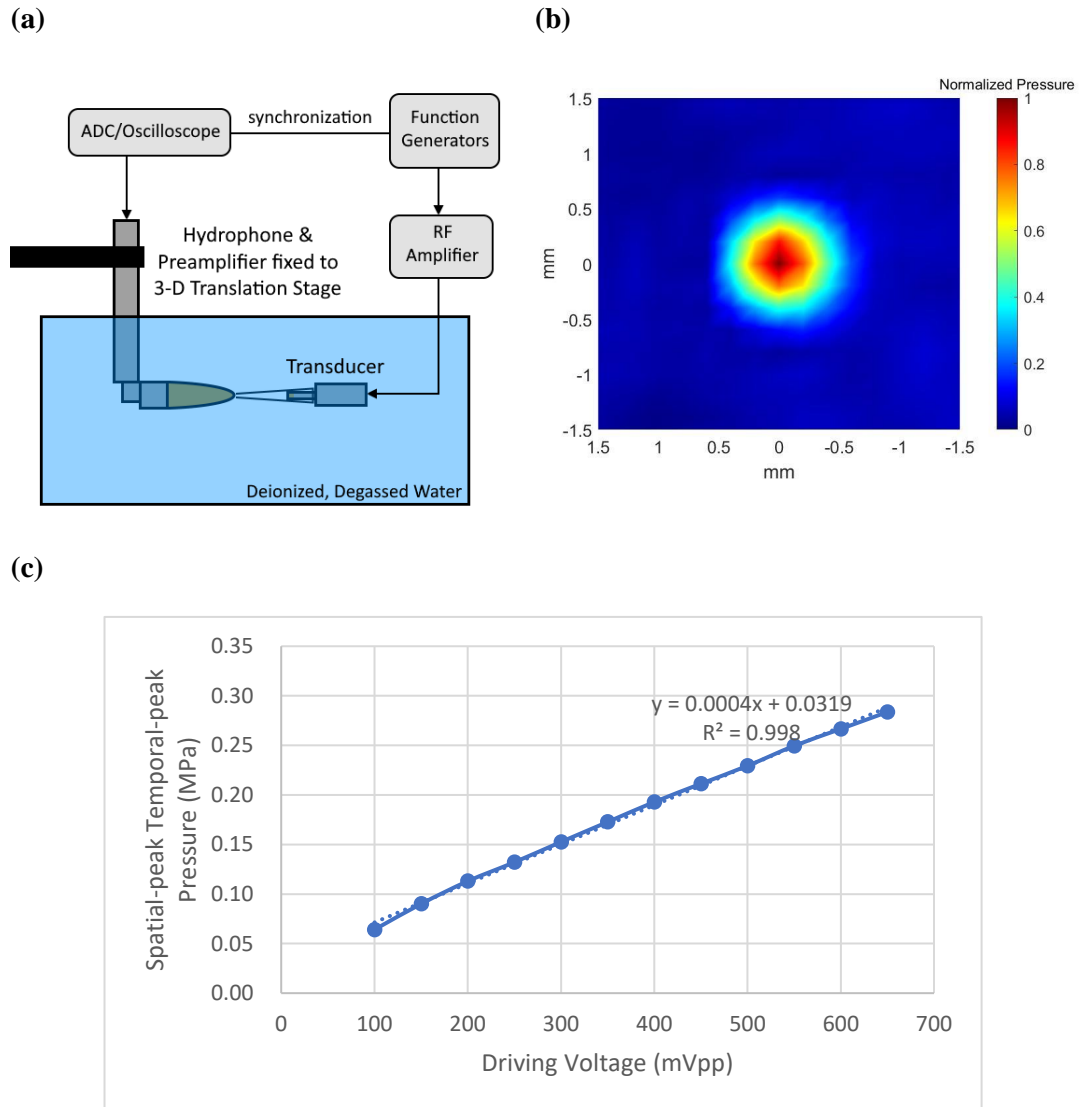


Figure 6. Acoustic output calibration of the confined transducer. **(a)** Schematic illustration of the detection setup; **(b)** Normalized acoustic profile; **(c)** Driving voltage input and corresponding acoustic output.

2.2.3 Ultrasound Stimulation Evaluation

Ultrasound trains were fired under continuous passive voltage-clamp recording. No typical waveform of ion channel opening induced inflow current (sudden drop in measured current) was observed. Yet, it was noticed a dose-dependent, low-frequency,

sinusoidal envelope was induced, in forms of spikes with varying baseline or spikes with varying amplitude.

We used the modified custom-made needle transducer to deliver bursts of ultrasonic wave. Single-tone bursts of 12 MHz sinusoidal wave were used to drive the ultrasound transducer. In the presented results, pulse width (t_1) was fixed to be 300 μs while other parameters: pulse interval (t_2), burst duration (t_3), burst interval (t_4) and spatial-peak temporal-peak acoustic pressure (P_{sptp}) are subject to be changed throughout the experiment. Representative waveforms were captured and presented below (Fig. 7a & 7b).

It can be concluded appearance of the envelope is correlated to transducer operation, likely an independent event of a sinusoidal waveform of period around 30s, gated by an ON/OFF pulse of 45 s interval, which was amplified by transducer operation (Fig. 8) in forms of spikes with varying baseline or spikes with varying amplitude, appearing in interval of around 10 ms. It is noticed that the temporal occurrence of such spikes is independent from transducer operating cycle, yet the aforementioned form of appearance seems to be correlated that with a longer t_2 (10 ms instead of 1 ms), spikes with varying amplitude are more likely to appear (Fig. 7f).

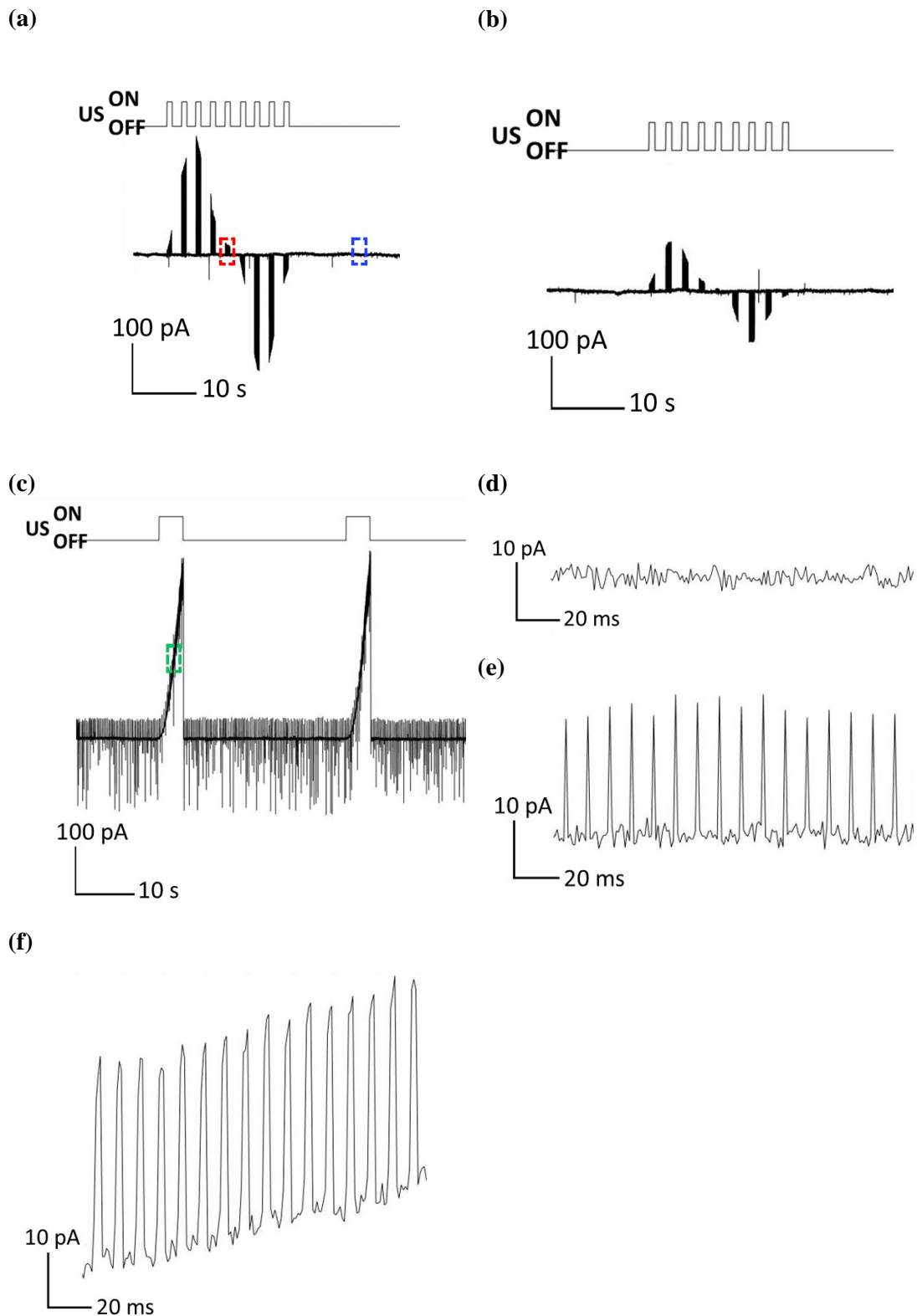


Figure 7. Unexpected sinusoidal ‘envelope’. **(a)** $t_2 = 10$ ms, $t_3 = 1$ s, $t_4 = 3$ s, $P_{\text{sptp}} = 0.15$ MPa; **(b)** $t_2 = 10$ ms, $t_3 = 1$ s, $t_4 = 3$ s, $P_{\text{sptp}} = 0.11$ MPa; **(c)** $t_2 = 1$ ms, $t_3 = t_4$, $P_{\text{sptp}} = 0.19$ MPa; **(d)** baseline signal from blue-framed area in **a**; **(e)** spikes from red-framed area in **a**; **(f)** spikes from green-framed area in **b**.

To eliminate potential signal contamination by function generator and power amplifier (50 dB nominal power gain) that drove the transducer, modification to recording setup was made: either by driving transducer directly with function generator, by-passing power amplifier, or operating transducer near but out of patch clamp recording chamber. Minimal effect can be observed in the former setting (Fig. 8a) but not in the latter (Fig. 8b), indicating the interaction was medium-mediated.

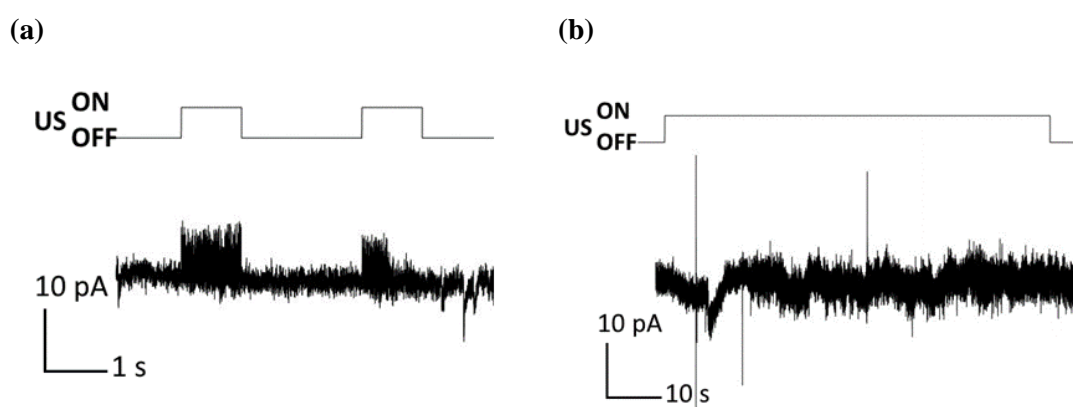


Figure 8. The induction of ‘envelope’ is medium-mediated. **(a)** 300 mVpp driving voltage (equivalent to 0.15 MPa) with amplifier OFF, $t_2 = 10$ ms, $t_3 = 1$ s, $t_4 = 3$ s; **(b)** transducer removed from recording chamber, $t_2 = 10$ ms, $t_3 = t_4$, $P_{\text{sptp}} = 0.19$ MPa.

2.3 Discussion

Using the prototype, no typical voltage-clamp waveform of ion channel opening induced inflow current (reduction in measured current) but a dose-dependent, low-frequency, sinusoidal envelope of repetitive spikes was observed, which to the author’s knowledge, has not been reported in journal articles. The ‘envelope’ phenomenon reported here, being regularly self-repeating and having long repetition rate, is not likely to be directly correlated to biological events, it might be outcome of previously unnoticed environmental factor, which might or might not affect experimental results.

It is also worth considering that, besides the generally noted 'leaky' sealing or sample damage, false positive ultrasound induced AP might be generated during patch clamp recording. Recent work by Collins and Mesce (2020) showed that by manually driven movements of the recording electrode in microns of spatial scales and seconds of temporal scale, similar characteristic waveform of membrane depolarization can be manipulated. Though the demonstrated effect was induced by movement of long temporal cycle, it raised the questions whether ultrasound induced depolarization recorded using patch clamp would be error raised by electrode movement or truly membrane depolarization. In the setting of this prototype, though ultrasound beam was confined and the giga-ohm seal remained after sonication, diameter of the main lobe at desired distance remained on submillimetre level that the glass pipette might still be under effect on a non-negligible scale. Until further understanding, it is suggested to avoid collecting patch clamp data directly from stimulation site. Investigators might utilize the intact neuronal circuit of *ex vivo* brain slices, by stimulating well-defined upstream brain region and collecting patch clamp data at corresponding downstream brain region, anatomically separated for a considerable distance. Animal treatment, brain slice preparation, and stimulation protocols shall be modified to ensure axon connection and area under effect of sonication, which shall be localized to the upstream brain region.

Chapter 3 Ultrasound Neuromodulation Platform Prototype II –

Stimulation through Neuronal Circuit

3.1 Materials and Methods

In this Chapter, a stimulation platform equipped with colocalized transducer-optical fibre complex was developed, aiming to spatially separate sonication and recording to different brain regions connected within a neural circuit. The addition of optical fibre served both as a visual guide and a potential light source for optogenetics integration. Classic dopamine reward circuit VTA-NAC was chosen for performance test. Brain slices were sensitized to ultrasound stimulation with mechanosensitive ion channel MscL at VTA; and were sensitized to optical stimulation with photosensitive ion channel ChR2 (Channelrhodopsin-2) at VTA via Cre-DIO system.

3.1.1 Ultrasound Stimulation Platform with Patch Clamp System

A 5-DoF micromanipulating platform for ultrasound transducer was constructed by assembling a 3-D manual micromanipulator (MM 33 with clamp, Märzhäuser Wetzlar, Germany), a 1-D goniometer (KSMG10-65, Zolix, China) and a rotation stage (RSM82-1A, Zolix, China) and fixed on a fixed stage microscope (BX51W1, Olympus, Japan) together with a motorized micromanipulator for patch clamp (MP-285, Sutter Instrument, USA). A multimode optical fibre was mounted on the side of the custom-made long needle transducer, near the ultrasound wave emitting end, which the lobe of fibre-delivered laser and the lobe of ultrasound beam colocalized at desired distance, under pre-determined angle of tilting.

3.1.2 Ultrasound Transducer Characterization

The custom-made long needle transducer was immersed in a large tank of deionized, degassed water, together with a hydrophone (HGL0200, ONDA, USA; preamplifier:

AG2010, ONDA, USA) installed on a 3-D translation stage (controller: XPS-D, Newport, USA; stage: M-ILS150CCHA, Newport, USA; XML210, Newport, USA). A combo of two function generators (Tektronix AFG3251, Agilent Technologies, USA; DG4102, Rigol, China) and a RF power amplifier (A075, Electronics & Innovation Ltd, USA) was used to drive the ultrasound transducers. To determine the driving voltage input and acoustic output relationship, the transducer was tilted at the pre-determined angle for optical-acoustic beam colocalization, then the hydrophone was aligned at a distance similar to that of the patch clamp experimental setup, waveforms under varying driving voltage were captured using oscilloscope (DS4024, Rigol, China) with matching input impedance; for the acoustic profile, upon finish of hydrophone-transducer alignment, a LabVIEW (National Instruments, USA) programme in sync with the function generators and an ADC board (PCI-5112, National Instruments, USA) was used to perform point-by-point 2D scanning of a pre-assigned area and step length. Waveforms at each scan point were captured and saved by the ADC board. In both tests, values of corresponding acoustic pressure were converted from the captured waveforms with pre-calibrated coefficient of hydrophone-preamplifier set provided by manufacturer.

3.1.3 Animal Treatment

C57BL/6 mice aged approximately 6 weeks were anesthetized with ketamine and xylazine (50 mg/kg and 15 mg/kg respectively) followed by shaving the skin above skull. Using a stereotaxic apparatus (RWD, China), craniotomy hole was drilled to allow injection. The coordinates used were AP -3.5 mm, ML 0.4 mm, DV -4.2 mm for VTA and AP 1.3 mm, ML 0.8 mm, DV -4.7 mm for NAC. Injection sites variously received 1 μ L of virus, VTA: psLenti-SFH-EGFP-P2A-PURO-CMV-MSCL-3xFLAG-WPRE and pAAV-Ef1a-DIO-hChR2(H134R)-mCherry; NAC: pAAV-

hSyn-EGFP-P2A-Cre-WPRE at 0.1 $\mu\text{L}/\text{min}$, followed by a 10-minute pause. The pipette was then retracted slowly, including a 5-minute pause at the halfway point. The puncture site was then disinfected and sutured, and the mice were returned to their housing areas for a recovery period no less than 3 weeks.

3.1.4 Brain Slices Preparation

Brain slices were prepared with reference to Ting et al. (2018): anesthetization was performed on the treated mice using ketamine and xylazine (50 mg/kg and 15 mg/kg respectively), followed by heart perfusion using NMDG-ACSF (92 mM NMDG, 2.5 mM KCl, 1.25 mM NaH_2PO_4 , 30 mM NaHCO_3 , 20 mM HEPES, 25 mM glucose, 5 mM sodium ascorbate, 2 mM thiourea, 3 mM sodium pyruvate, 10 mM MgSO_4 , 0.5 mM CaCl_2 , pH 7.3~7.4 using HCl). Animal euthanasia was performed by cervical dislocation. Brains were then quickly removed and chilled in ice-cold NMDG ACSF well oxygenated with 95% O_2 + 5% CO_2 . Sagittal slices (300 μm) were then cut using a semiautomatic vibrating blade microtome (VT1200, Leica Biosystems, USA) and subsequently incubated for 10 minutes at 35°C. The slices were then transferred to a light-shielding storage chamber filled with oxygenated holding ACSF (92 mM NaCl, 2.5 mM KCl, 1.25 mM NaH_2PO_4 , 30 mM NaHCO_3 , 20 mM HEPES, 25 mM glucose, 5 mM sodium ascorbate, 2 mM thiourea, 3 mM sodium pyruvate, 2 mM CaCl_2 , 2 mM MgSO_4 , pH 7.3–7.4 using NaOH, oxygenated with 95% O_2 + 5% CO_2) at room temperature. A recovery period no less than 60 minutes was allowed before patch clamp recordings.

3.1.5 Fluorescence Imaging

To confirm ion channel expression, fluorescence imaging was performed under microscope (BX51WI, Olympus, Japan; digital camera: 01-PRIME-BSI-EXP,

Teledyne Photometrics, USA) right before patch clamp recording. White light source (Sola 80-10068, Lumencor Light Engine, USA) was filtered accordingly and resulting image was saved with pseudo colour addition.

3.1.6 Electrophysiology Recording (Patch Clamp)

Glass pipettes used were pulled from glass capillary tube (Vitrex, Modulohm A/S, Denmark) using Flaming/Brown micropipette puller (P-1000, Sutter Instrument, USA). The pipettes were filled with internal solution (138 mM KCl, 10 mM NaCl, 1 mM MgCl₂, 10 mM HEPES with D-manitol compensated for 290 mOsm) prior patch clamp recordings. Patch clamp recordings were done using HEKA patch clamp system (EPC 10 USB, HEKA Elektronik, Germany; software: PATCHMASTER, HEKA Elektronik, Germany) under visual aid of differential interference contrast microscopy (BX51WI, Olympus, Japan; digital camera: 01-PRIME-BSI-EXP, Teledyne Photometrics, USA). Brain slices were bathed in recording ACSF (124 mM NaCl, 2.5 mM KCl, 1.25 mM NaH₂PO₄, 24 mM NaHCO₃, 12.5 mM glucose, 2 mM CaCl₂, and 2 mM MgSO₄, oxygenated with 95% O₂ + 5% CO₂) under perfusion. Brain region was identified by visual inspection and cell type was confirmed by characteristic waveforms under voltage step stimulation (-100 mV to 100 mV). After formation of whole-cell giga-ohm seal, holding voltage was set at -60mv. Cell activities in term of inward current were recorded using continuous passive voltage-clamp under gap-free recording mode and sampling rate 10 kHz.

3.1.7 Ultrasound Stimulation

To evaluate effect of ultrasound stimulation, the transducer was placed, tilted with the pre-determined angle, pointing to the well-defined upstream brain region VTA with the help of fibre-delivered laser, driven by laser light source (465 nm, Inper, China) at

intensity posing negligible bioeffect to neurons. The same combo of two function generators (Tektronix AFG3251, Agilent Technologies, USA; DG4102, Rigol, China) and a RF power amplifier (A075; Electronics & Innovation Ltd, USA) as in ultrasound transducer calibration was used to drive the ultrasound transducers, generating single-tone bursts of varying spatial-peak temporal-peak acoustic pressure (P_{sptp}), pulse width (t_1), pulse interval (t_2), burst duration (t_3), and burst interval (t_4).

3.2 Results

3.2.1 Ultrasound Transducer Characterization

To quantify the acoustic output, hydrophone measurement was performed in a large tank of deionized, degassed water (Fig. 9a). Point-by-point 2D measurement of acoustic output of the customized transducer was firstly measured along propagation direction. Resulting acoustic profile (Fig. 9b, top), together with optical fibre performance data provided by manufacturer, was examined to determine tilting angle for ultrasound-laser colocalization. Another 2D scan (Fig. 9b, bottom) was performed on the expected plane where tissue sample would be located (dotted line in Fig. 9a) after adjusting the transducer-hydrophone alignment accordingly. Single-point measurement (Fig. 9c) was later carried out at the centre of acoustic beam to map driving voltage to P_{sptp} .

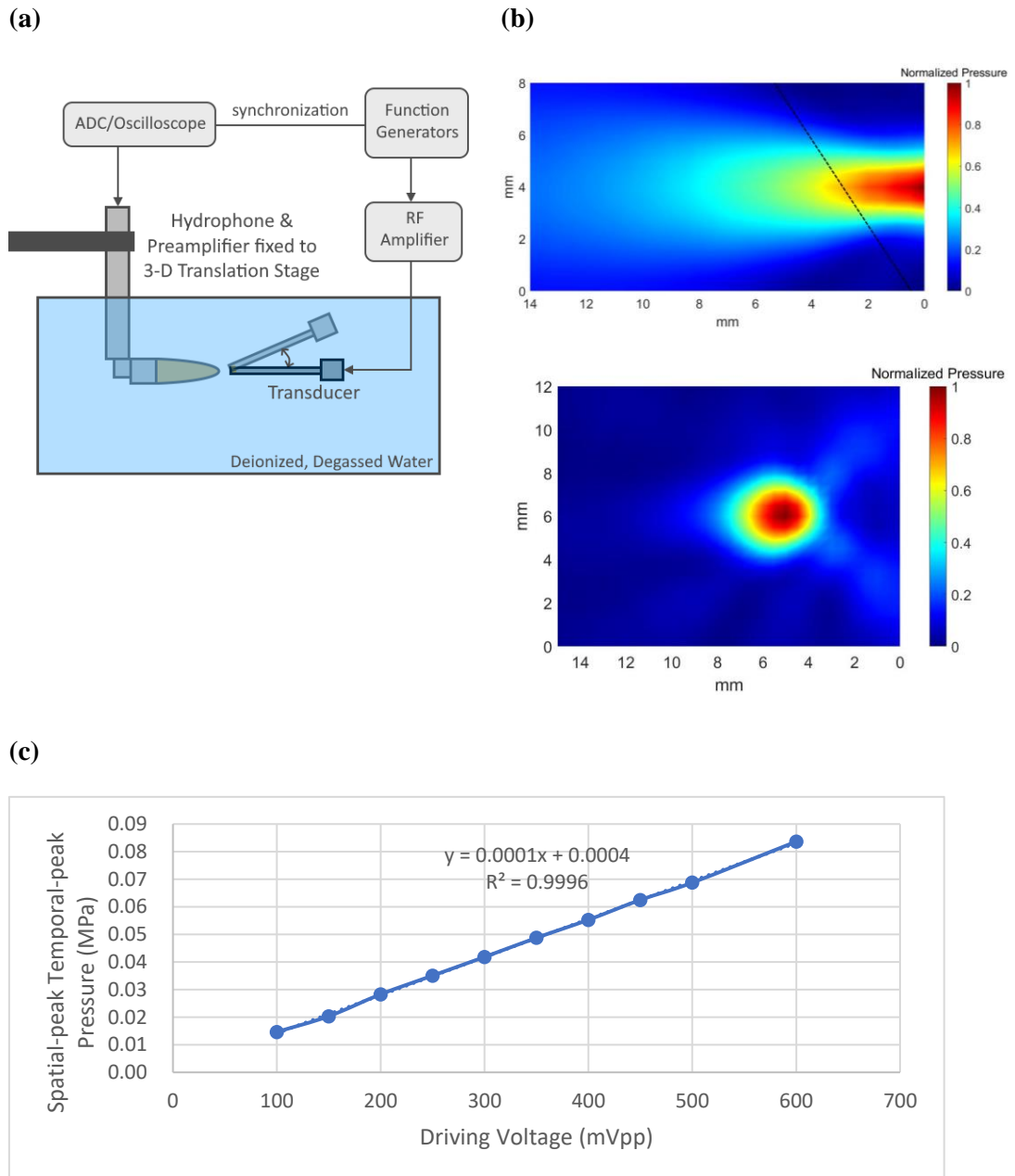


Figure 9. Acoustic output calibration of the custom-made needle transducer. **(a)** Schematic illustration of the detection setup; **(b)** Normalized acoustic profile. (top) Along propagation direction; (bottom) On expected tilted plane (indicated as dotted line at top figure); **(c)** Driving voltage input and corresponding acoustic output;

3.2.2 Ultrasound Stimulation Platform with Patch Clamp System

Since alignment of the ultrasound transducer greatly influence the acoustic profile at the recording chamber, to maximize tunability of the system, a 5 degree-of-freedom

(DoF) micromanipulating platform for ultrasound transducer that allows manual fine-tuning in linear translation along x-, y- and z-axes, and rotation about y- and z-axes was constructed (Fig. 10a). In order to facilitate precise alignment, an optical fibre was attached to the transducer as a ‘visual guide’.

To set the system for experimental validation, the transducer was tilted to avoid standing wave, which could alter the acoustic pressure at a certain point from near zero to up to double the original value; and allow transducer-laser colocalization as described in Chapter 3.2.1 (Fig. 10d).

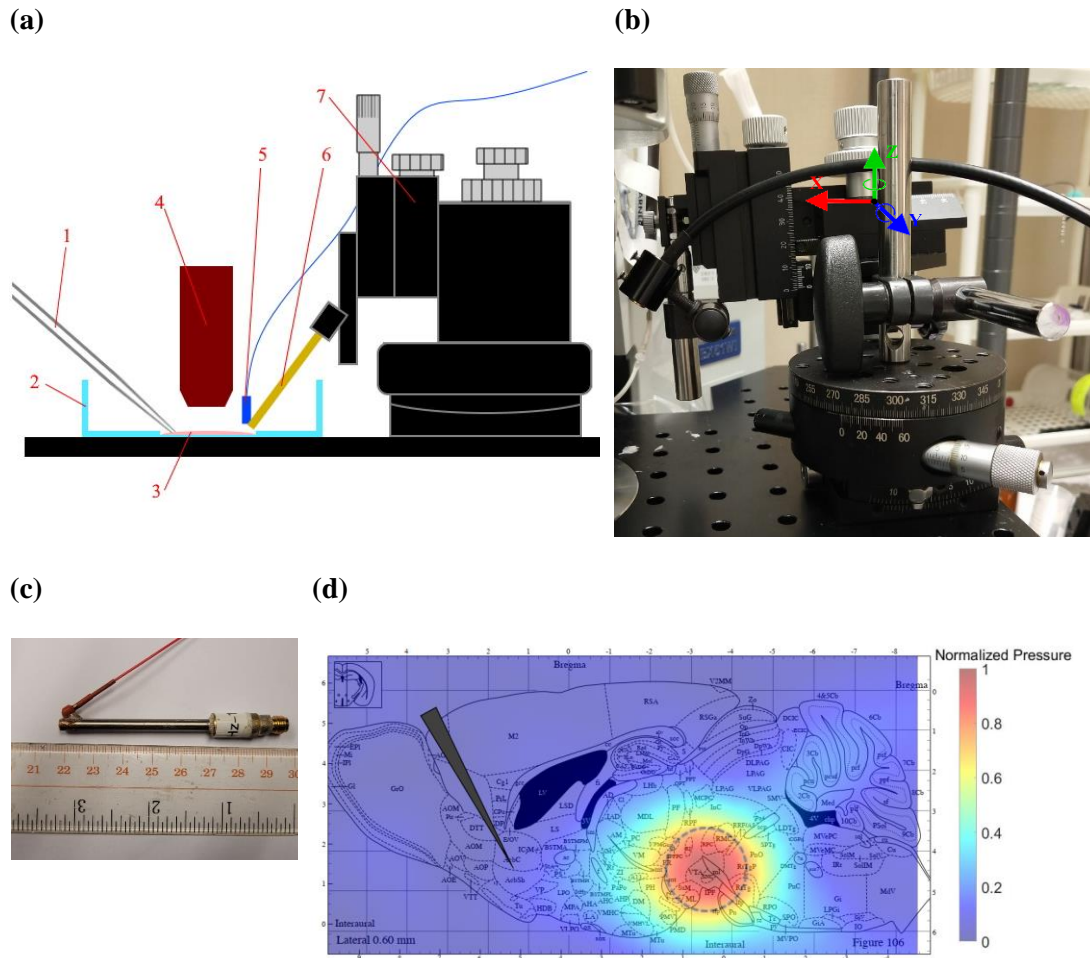


Figure 10. The developed ‘circuit’ ultrasound stimulation platform prototype. **(a)** Schematic illustration of the developed system. (1) patch pipette; (2) record chamber modified from confocal dish; (3) tissue sample (brain slice); (4) microscope objective; (5) optical fibre; (6) ultrasound transducer; (7) 5-DoF micromanipulating platform; **(b)** Demonstration of the 5-DoF micromanipulating platform; **(c)** Demonstration of the custom-made needle transducer; **(d)** Illustration of ultrasound and laser beam profile and patch site, overlaid on sample brain slice drawing. Heat map: ultrasound; dashed circle: laser; triangle: patch clamp glass pipette.

(d) Modified from “The Mouse Brain in Stereotaxic Coordinates”, by Paxinos, G., & Franklin, K. B., 2004, p. 156, Houston, Texas: Gulf Professional Publishing; and Figure 9b, bottom

3.2.3 Ultrasound Stimulation Evaluation

Neurons were sensitized to ultrasound stimulation by transfecting MscL (large-conductance mechanosensitive ion channel), labelled with EGFP (enhanced green fluorescent protein). Cell body of neurons can be clearly seen under fluorescence for EGFP (Fig. 11), indicating the successful transfection of viral vector and thus expression of MscL, functionalizing the neurons to mechanical stimuli, which in this work, provided by ultrasound stimulation.

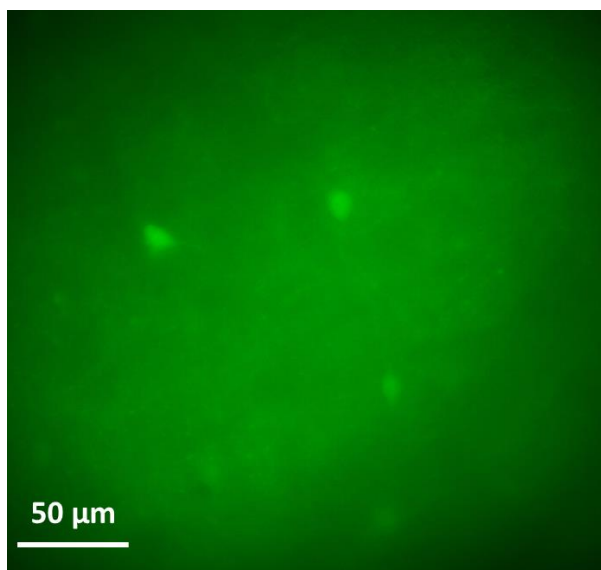


Figure 11. Fluorescence image of EGFP (MscL) at VTA region.

To establish a ‘circuit’ stimulation strategy, we chose a well-known dopamine reward circuitry VTA-NAC (Ikemoto, 2007), spatially separated by around 5 mm, which was far enough under our setting to minimize direct ultrasonic interference to patch clamp recording (Fig. 10d). To validate our proposed stimulation strategy, we first performed sonication and patch clamp recording on the same site, at NAC and VTA region respectively. Ultrasound trains were fired under continuous passive voltage-clamp recording, targeting VTA region under visual aid of low-power laser delivered from assembled optical fibre. Slight interference was introduced to the

system when targeting unsensitized NAC region but no ion channel activation was observed (Fig. 12); where dose-dependent responses were captured when targeting sensitized VTA region (Fig. 13), further indicating functional expression of MscL.

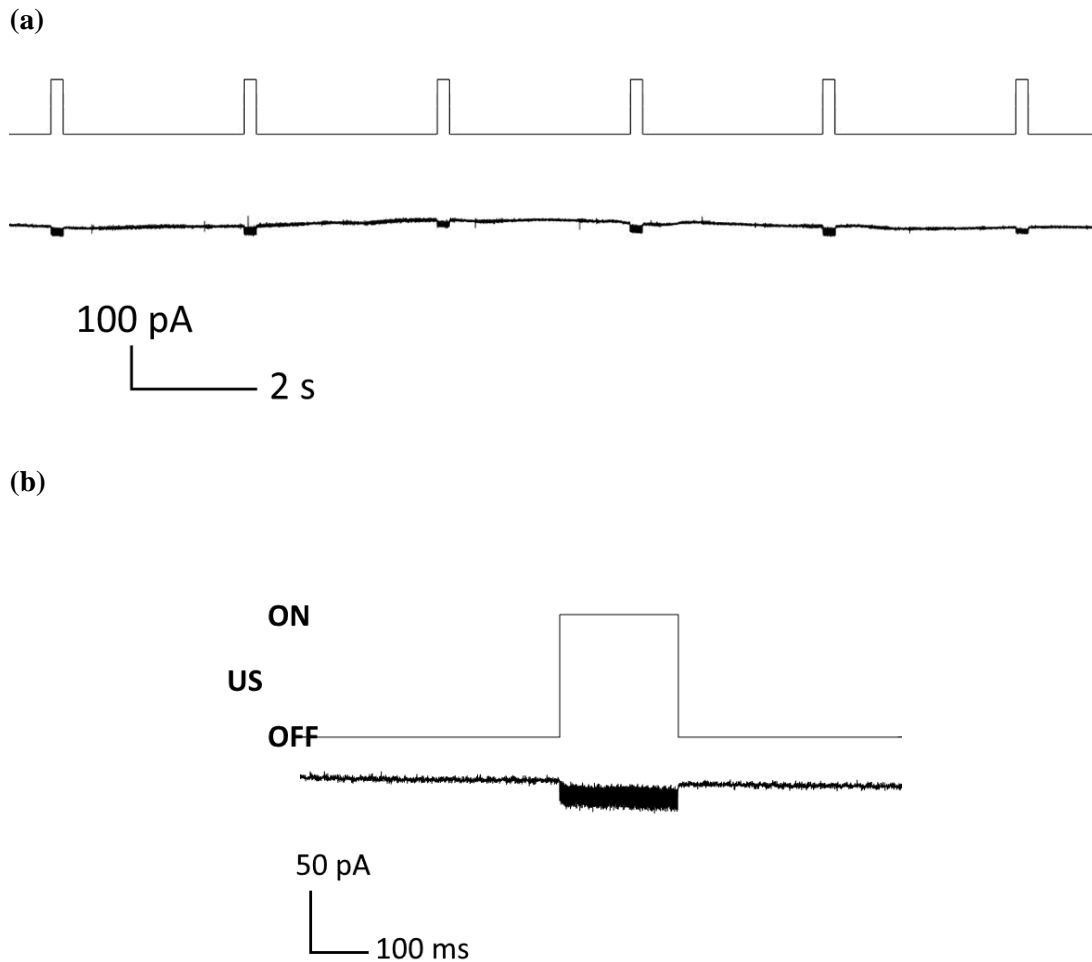


Figure 12. No observable ion channels activation by ultrasound under same site recording at NAC. Here, $t_1 = 200 \mu\text{s}$, $t_2 = 1 \text{ ms}$, $t_3 = 200 \text{ ms}$, $t_4 = 7\text{s}$, $P_{\text{sptp}} = 0.24 \text{ MPa}$ (a) Representative patch clamp recording sequence; (b) Representative response under single burst cycle extracted from (a).

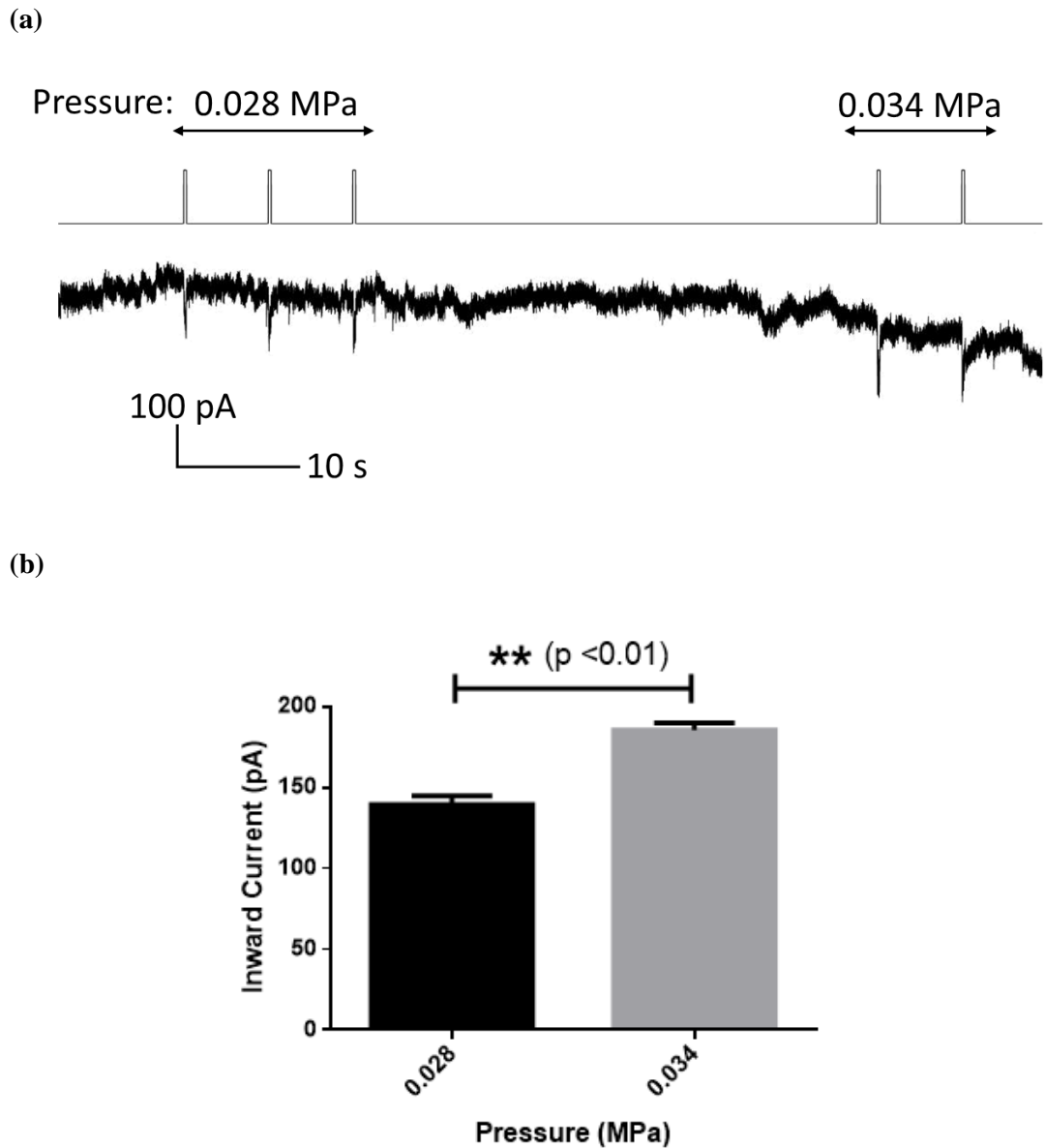


Figure 13. Ion channels activated by ultrasound under same site recording at VTA. Here, $t_1 = 200 \mu\text{s}$, $t_2 = 1 \text{ ms}$, $t_3 = 200 \text{ ms}$, $t_4 = 3\text{s}$. (a) Representative patch clamp recording sequence under varying P_{sptp} ; (b) Inward current quantification ($n = 3$).

The setup was then re-aligned that sonication was delivered to VTA region and patch clamp recording was performed at NAC region. Inward current showing trend of dose dependency was captured (Fig. 14).

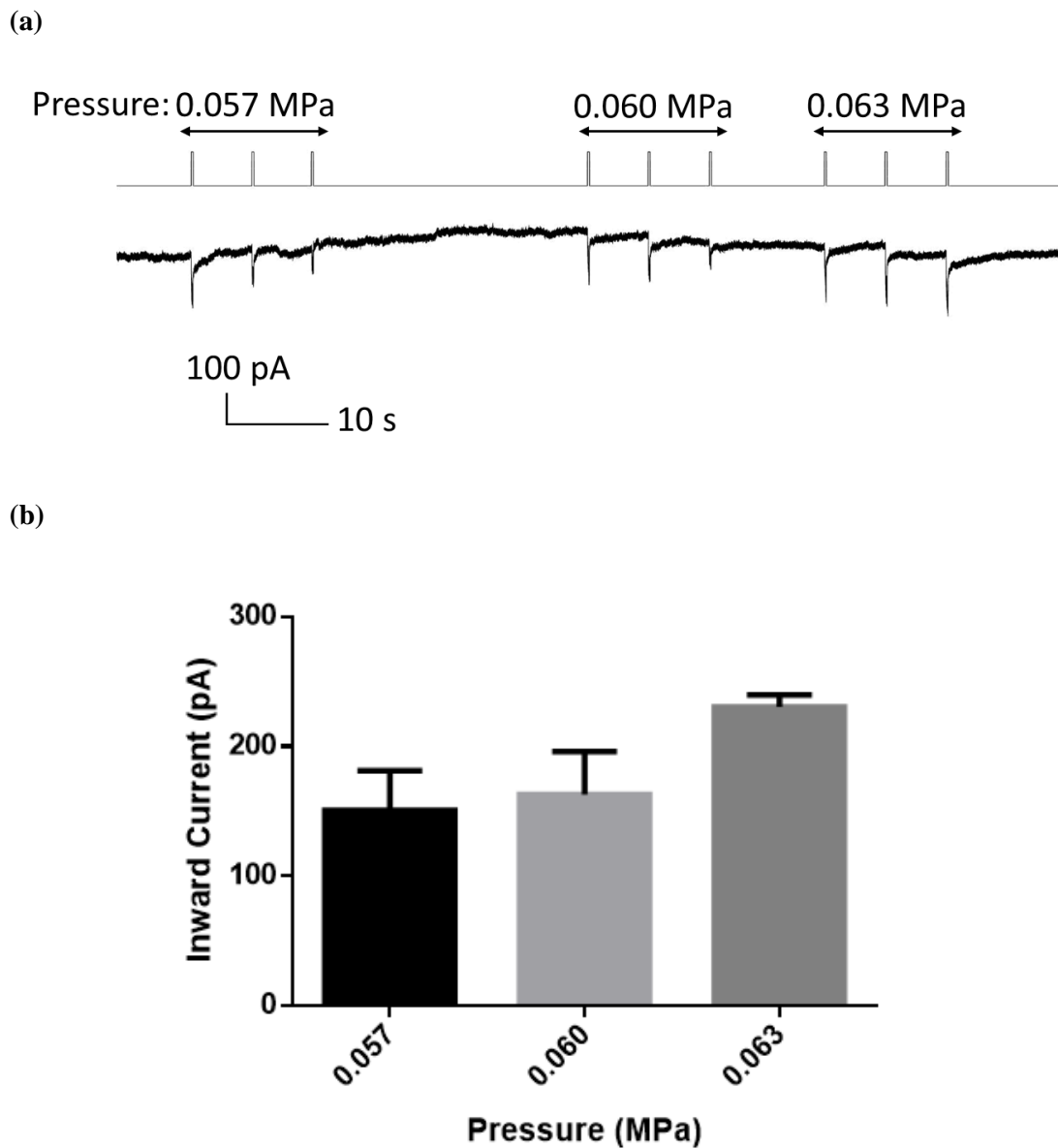


Figure 14. Ion channels activated by ultrasound via ‘circuit’ strategy (sonication at VTA, patch clamp recording at NAC). Here, $t_1 = 200 \mu\text{s}$, $t_2 = 1 \text{ ms}$, $t_3 = 200 \text{ ms}$, $t_4 = 7 \text{ s}$. (a) Representative patch clamp recording sequence under varying P_{sftp} ; (b) Inward current quantification ($n = 3$).

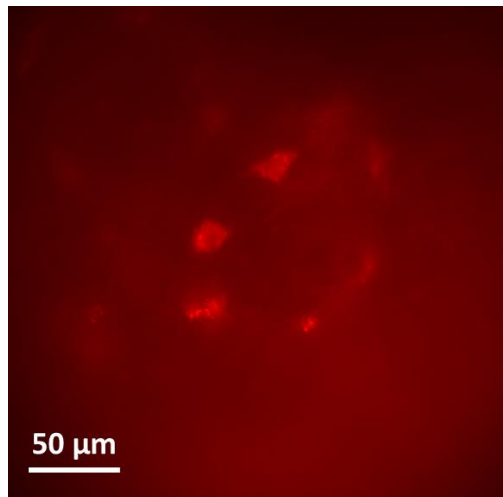
Taken together, ion channel activation was observed at sensitized VTA region but not unsensitized NAC region, indicating response captured via ‘circuit’ stimulation strategy (Fig. 14) was not induced by direct effect of ultrasound on recording site.

Furthermore, when comparing the quantifications of inward current induced by sonication at VTA region (Fig. 13b & 14b), similar current amplitude was captured at VTA under smaller pressure than that at NAC, suggesting VTA activation a more primary response. Thus, suggesting the prototype is capable of ultrasound neuromodulation investigation.

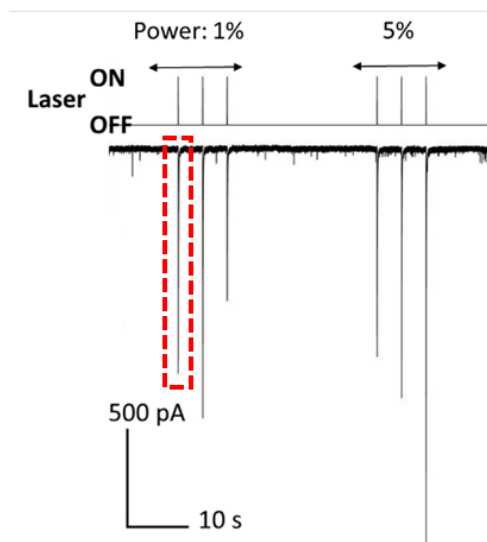
3.2.4 Optical Stimulation Evaluation

In addition to MscL, neurons in VTA region were also transfected with ChR2, a photosensitive nonspecific cation channel, labelled with fluorophore mCherry. Cell body of neurons can be clearly seen under fluorescence for mCherry (Fig. 15a), indicating the successful transfection of viral vector and thus expression of ChR2, functionalizing the neurons to optical stimuli, which in this work, provided by laser delivered through optical fibre. We then confirmed the function of ChR2 expressing neurons by same site stimulation and patch clamp recording at VTA region (Fig. 15b & c), results indicating a successful sensitization and suggesting the prototype is capable of optogenetics investigation.

(a)



(b)



(c)

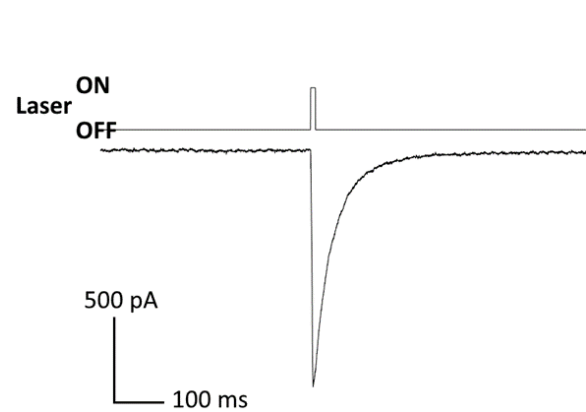


Figure 15. Sensitization of neurons at VTA to optical stimulation. **(a)** Fluorescence image of mCherry (ChR2) at VTA region. **(b)** Representative patch clamp recording sequence. Here, power 1% = intensity 0.806 W/cm^2 , $t_1 = 10 \text{ ms}$, $t_2 = 4\text{s}$; **(c)** Representative response under single laser pulse extracted from red-framed region in **b**.

3.3 Discussion

Taken the data together (Fig. 12 – 14), the developed prototype is able to serve as a ultrasound neuromodulation platform of satisfactory performance, yet several

improvement and optimization are available. First, the laser-ultrasound colocalization is valid only within millimetre, though the technique is universally translatable in development phase, the system failed to be a universal investigation tool across platform once established. Yet, patch clamp system is highly vulnerable to environmental noise that it is not recommended to modify setting much once established, we believe the current prototype is satisfactory for most investigation context; second, we tried to implement Cre-DIO (double-floxed inverse open reading frame) system with ChR2 but yet to be optimal. By transfecting ‘Cre’ at downstream brain region and ‘DIO’ at upstream brain region, reporter gene at upstream brain region would only be expressed in the presence of ‘Cre’, thus ensuring neural connection once reporter gene is expressed. Ideally, ChR2 and MscL would be co-expressed on neurons in VTA region that, on one hand, ensures neural connectivity for ‘circuit’ stimulation; on the other hand, sensitizes the neuron to both optical and ultrasound stimulation, providing opportunity to compare and contrast ultrasound neuromodulation with optogenetics on exact setting. Our results showed laser delivered by the assembled optical fibre, with increased intensity than that used for visual aid, was able to induce ChR2 response (Fig. 15b), yet ChR2-MscL co-expression was unsatisfactory (data not shown) and no response in patch clamp recording could be captured at NAC through same ‘circuit’ strategy, indicating the need to polish the animal treatment and brain slice preparation protocol.

Though sample size was low for statistically significant conclusion, it is worth noticing that dose dependency can be observed under same site stimulation strategy but not significant under ‘circuit’ stimulation strategy (Fig. 13b & 14b), while in general, ultrasound stimulation has been reported to show dose dependency *in vivo*, *in vitro* and *ex vivo*. One possible explanation is limitation by acoustic pressure range used in this study that single cell response through our ‘circuit’ strategy has been saturated or the

dose dependent change cannot be resolved; another possible explanation is confounds raised by investigation methods. Most works on ultrasound stimulation either evaluates direct cell response under stimulation (equivalent to our 'direct' stimulation strategy), such as Ca^{2+} influx at target region(Qiu et al., 2019; Qiu et al., 2020); or circuitry response of intact brain, such as behavioural motor response (Qiu et al., 2020) and endocrinal response (Xian et al., 2021). The neuronal connection might be disrupted in our brain slice samples that the sensitivity of neurons at NAC region to upstream signalling was reduced and thus, the dose dependent change cannot be resolved.

Chapter 4 Conclusion

In this study, prototypes adopting ‘direct’ and ‘circuit’ ultrasound stimulation strategy respectively were developed, which the ‘direct’ stimulation prototype possibly revealed a previously unreported ‘envelope’ phenomenon that might reduce repeatability and reliability of *ex vivo* patch clamp results; and the ‘circuit’ stimulation prototype was demonstrated to be able to serve as a ultrasound neuromodulation platform of satisfactory performance, with potential to integrate optogenetics and ultrasound neuromodulation into a single setup. The development of ultrasound neuromodulation platform is not necessary to be universally applicable to research contexts as a product but to serve as a protocol for investigators to adapt to own setups. The aim of this study, “to develop an ultrasound neuromodulation platform for precise neuronal stimulation and real-time multi-modal monitoring, as a standardized protocol and/or method”, is achieved with rooms for further improvement and optimization.

References

- Andrés, R. R., Acosta, V. M., & Riera, E. (2017). *Ultrasonic field generated by different airborne power ultrasonic transducers with extensive radiators*. Paper presented at the Tecniacústica 2017: 48º Congreso Español de Acústica; Encuentro Ibérico de Acústica; European Symposium on Underwater Acoustics Applications; European Symposium on Sustainable Building Acoustics: A Coruña 3-6 Octubre 2017.
- Baek, H., Pahk, K. J., & Kim, H. (2017). A review of low-intensity focused ultrasound for neuromodulation. *Biomedical Engineering Letters*, 7(2), 135-142.
- Bijsterbosch, J. D., Barker, A. T., Lee, K.-H., & Woodruff, P. W. (2012). Where does transcranial magnetic stimulation (TMS) stimulate? Modelling of induced field maps for some common cortical and cerebellar targets. *Medical & biological engineering & computing*, 50(7), 671-681.
- Blackmore, J., Shrivastava, S., Sallet, J., Butler, C. R., & Cleveland, R. O. (2019). Ultrasound neuromodulation: a review of results, mechanisms and safety. *Ultrasound in medicine & biology*, 45(7), 1509-1536.
- Brown, T. D. (2000). Techniques for mechanical stimulation of cells in vitro: a review. *Journal of biomechanics*, 33(1), 3-14.
- Chang, C.-H., Lane, H.-Y., & Lin, C.-H. (2018). Brain stimulation in Alzheimer's disease. *Frontiers in psychiatry*, 9, 201.
- Chen, R., Gore, F., Nguyen, Q.-A., Ramakrishnan, C., Patel, S., Kim, S. H., . . . Krook-Magnusson, E. (2021). Deep brain optogenetics without intracranial surgery. *Nature biotechnology*, 39(2), 161-164.
- Collins, M. N., & Mesce, K. A. (2020). Focused Ultrasound Neuromodulation and the Confounds of Intracellular Electrophysiological Investigation. *eNeuro*, 7(4), ENEURO.0213-0220.2020. doi:10.1523/ENEURO.0213-20.2020
- Dallapiazza, R. F., Timbie, K. F., Holmberg, S., Gatesman, J., Lopes, M. B., Price, R. J., . . . Elias, W. J. (2017). Noninvasive neuromodulation and thalamic mapping with low-intensity focused ultrasound. *Journal of neurosurgery*, 128(3), 875-884.
- de Asis Jr, E. D., Leung, J., Wood, S., & Nguyen, C. V. (2009). High spatial resolution single multiwalled carbon nanotube electrode for stimulation, recording, and whole cell voltage clamping of electrically active cells. *Applied Physics Letters*, 95(15), 153701.
- Deisseroth, K., Feng, G., Majewska, A. K., Miesenböck, G., Ting, A., & Schnitzer, M. J. (2006). Next-generation optical technologies for illuminating genetically targeted brain circuits. *Journal of Neuroscience*, 26(41), 10380-10386.
- Duke, A. R., Jenkins, M. W., Lu, H., McManus, J. M., Chiel, H. J., & Jansen, E. D. (2013). Transient and selective suppression of neural activity with infrared light. *Scientific reports*, 3(1), 1-8.
- Eaton, H. (1991). Magnetic Nerve Stimulation. *Johns Hopkins AFL Technical Digest*, 12(2), 153-158.
- Focused Ultrasound Foundation. (2015). An Overview of the Biological Effects of Focused Ultrasound.
- Fowler, M., Cotter, J., Knight, B., Sevic-Muraca, E., Sandberg, D., & Sirianni, R. (2020). Intrathecal drug delivery in the era of nanomedicine. *Advanced drug delivery reviews*, 165, 77-95.
- Guleyupoglu, B., Schestatsky, P., Edwards, D., Fregni, F., & Bikson, M. (2013). Classification of methods in transcranial electrical stimulation (tES) and evolving strategy from historical approaches to contemporary innovations. *Journal of neuroscience methods*, 219(2), 297-311.
- Harvey, E. N. (1929). The effect of high frequency sound waves on heart muscle and other irritable tissues. *American Journal of Physiology-Legacy Content*, 91(1), 284-290.
- Horn, R., & Marty, A. (1988). Muscarinic activation of ionic currents measured by a new whole-cell recording method. *The Journal of general physiology*, 92(2), 145-159.

- Ikemoto, S. (2007). Dopamine reward circuitry: two projection systems from the ventral midbrain to the nucleus accumbens–olfactory tubercle complex. *Brain research reviews*, *56*(1), 27-78.
- Janssen, A. M., Oostendorp, T. F., & Stegeman, D. F. (2014). The effect of local anatomy on the electric field induced by TMS: evaluation at 14 different target sites. *Medical & biological engineering & computing*, *52*(10), 873-883.
- Kamimura, H. A., Conti, A., Toschi, N., & Konofagou, E. E. (2020). Ultrasound neuromodulation: Mechanisms and the potential of multimodal stimulation for neuronal function assessment. *Frontiers in physics*, *8*, 150.
- Kubanek, J., Shukla, P., Das, A., Baccus, S. A., & Goodman, M. B. (2018). Ultrasound elicits behavioral responses through mechanical effects on neurons and ion channels in a simple nervous system. *Journal of Neuroscience*, *38*(12), 3081-3091.
- Lee, W., Lee, S. D., Park, M. Y., Foley, L., Purcell-Estabrook, E., Kim, H., . . . Yoo, S.-S. (2016). Image-guided focused ultrasound-mediated regional brain stimulation in sheep. *Ultrasound in medicine & biology*, *42*(2), 459-470.
- Lin, Z., Zhou, W., Huang, X., Wang, K., Tang, J., Niu, L., . . . Zheng, H. (2018). On-chip ultrasound modulation of pyramidal neuronal activity in hippocampal slices. *Advanced Biosystems*, *2*(8), 1800041.
- Lipovsek, M., Bardy, C., Cadwell, C. R., Hadley, K., Kobak, D., & Tripathy, S. J. (2021). Patch-seq: Past, present, and future. *Journal of Neuroscience*, *41*(5), 937-946.
- Neher, E., & Sakmann, B. (1976). Single-channel currents recorded from membrane of denervated frog muscle fibres. *Nature*, *260*(5554), 799-802.
- Neher, E., & Sakmann, B. (1991). The Nobel Prize in Physiology or Medicine 1991.
- Neher, E., & Sakmann, B. (1992). The Patch Clamp Technique. *Scientific American*, *266*(3), 44-51. Retrieved from <http://www.jstor.org/stable/24938980>
- Obergrussberger, A., Friis, S., Brüggemann, A., & Fertig, N. (2021). Automated patch clamp in drug discovery: major breakthroughs and innovation in the last decade. In (Vol. 16, pp. 1-5): Taylor & Francis.
- Oh, S.-J., Lee, J. M., Kim, H.-B., Lee, J., Han, S., Bae, J. Y., . . . Hwang, E.-S. (2019). Ultrasonic neuromodulation via astrocytic TRPA1. *Current Biology*, *29*(20), 3386-3401. e3388.
- Pardridge, W. M. (2011). Drug transport in brain via the cerebrospinal fluid. *Fluids and Barriers of the CNS*, *8*(1), 1-4.
- Park, D.-W., Ness, J. P., Brodnick, S. K., Esquibel, C., Novello, J., Atry, F., . . . Swanson, K. I. (2018). Electrical neural stimulation and simultaneous in vivo monitoring with transparent graphene electrode arrays implanted in GCaMP6f mice. *ACS nano*, *12*(1), 148-157.
- Pastrana, E. (2011). Optogenetics: controlling cell function with light. *Nature Methods*, *8*(1), 24-25.
- Paviolo, C., & Stoddart, P. R. (2017). Gold nanoparticles for modulating neuronal behavior. *Nanomaterials*, *7*(4), 92.
- Paxinos, G., & Franklin, K. B. (2004). *The Mouse Brain in Stereotaxic Coordinates*: Gulf Professional Publishing.
- Prieto, M. L., Firouzi, K., Khuri-Yakub, B. T., & Maduke, M. (2018). Activation of Piezo1 but not NaV1. 2 channels by ultrasound at 43 MHz. *Ultrasound in medicine & biology*, *44*(6), 1217-1232.
- Qiu, Z., Guo, J., Kala, S., Zhu, J., Xian, Q., Qiu, W., . . . Zhang, R. (2019). The mechanosensitive ion channel Piezo1 significantly mediates in vitro ultrasonic stimulation of neurons. *Iscience*, *21*, 448-457.
- Qiu, Z., Kala, S., Guo, J., Xian, Q., Zhu, J., Zhu, T., . . . Wang, H. (2020). Targeted neurostimulation in mouse brains with non-invasive ultrasound. *Cell Reports*, *32*(7), 108033.
- Rezayat, E., & Toostani, I. G. (2016). A review on brain stimulation using low intensity focused ultrasound. *Basic and clinical neuroscience*, *7*(3), 187.

- Richter, C. P., Matic, A. I., Wells, J. D., Jansen, E. D., & Walsh, J. T. (2011). Neural stimulation with optical radiation. *Laser & photonics reviews*, 5(1), 68-80.
- Rosa, M. A., & Lisanby, S. H. (2012). Somatic treatments for mood disorders. *Neuropsychopharmacology*, 37(1), 102-116.
- Rossini, P. M., Burke, D., Chen, R., Cohen, L., Daskalakis, Z., Di Iorio, R., . . . George, M. (2015). Non-invasive electrical and magnetic stimulation of the brain, spinal cord, roots and peripheral nerves: basic principles and procedures for routine clinical and research application. An updated report from an IFCN Committee. *Clinical neurophysiology*, 126(6), 1071-1107.
- Sassaroli, E., & Vykhodtseva, N. (2016). Acoustic neuromodulation from a basic science prospective. *Journal of therapeutic ultrasound*, 4(1), 1-14.
- Shealy, C. N., & Henneman, E. (1962). Reversible effects of ultrasound on spinal reflexes. *Archives of neurology*, 6(5), 374-386.
- Ting, J. T., Lee, B. R., Chong, P., Soler-Llavina, G., Cobbs, C., Koch, C., . . . Lein, E. (2018). Preparation of acute brain slices using an optimized N-methyl-D-glucamine protective recovery method. *JoVE (Journal of Visualized Experiments)*(132), e53825.
- Tyler, W. J., Tufail, Y., Finsterwald, M., Tauchmann, M. L., Olson, E. J., & Majestic, C. (2008). Remote excitation of neuronal circuits using low-intensity, low-frequency ultrasound. *PloS one*, 3(10), e3511.
- Wang, P., Zhang, J., Yu, J., Smith, C., & Feng, W. (2019). Brain modulatory effects by low-intensity transcranial ultrasound stimulation (TUS): a systematic review on both animal and human studies. *Frontiers in neuroscience*, 13, 696.
- Wang, S., Meng, W., Ren, Z., Li, B., Zhu, T., Chen, H., . . . Jiang, H. (2020). Ultrasonic Neuromodulation and Sonogenetics: A New Era for Neural Modulation. *Frontiers in Physiology*, 11.
- Xian, Q., Qiu, Z., Kala, S., Wong, K. F., Murugappan, S., Wu, Y., . . . Sun, L. (2021). Circuit-specific sonogenetic stimulation of the deep brain elicits distinct signaling and behaviors in freely moving mice. *bioRxiv*.
- Yang, C., & Park, S. (2021). Nanomaterials-assisted thermally induced neuromodulation. *Biomedical Engineering Letters*, 1-8.
- Yavari, F., Jamil, A., Samani, M. M., Vidor, L. P., & Nitsche, M. A. (2018). Basic and functional effects of transcranial electrical stimulation (tES)—an introduction. *Neuroscience & Biobehavioral Reviews*, 85, 81-92.
- Young, R. R., & Henneman, E. (1961). Reversible block of nerve conduction by ultrasound: Ultrasonic blocking of nerve fibers. *Archives of neurology*, 4(1), 83-89.